Rhodium Complexes with Tripodal Polyphosphines as Excellent Precursors to Systems for the Activation of H-H and C-H Bonds

Claudio Bianchini,* Dante Masi, Andrea Meli, Maurizio Peruzzini, and Fabrizio Zanobini

Contribution from the Istituto per lo Studio della Stereochimica ed Energetica dei Composti di Coordinazione, C.N.R., Via J. Nardi 39, Florence 50132, Italy. *Received October 26, 1987*

Abstract: The trigonal-bipyramidal (TBP) Rh(I) complexes $[(NP_3)RhCl]$ (**1**) and $[(PP_3)RhCl]$ (**2**) are protonated by strong acids to give, after addition of $NaBPh_4$, the octahedral (OCT) *cis*-(chloride)hydrides $[(NP_3)Rh(H)Cl]BPh_4$ (**3**) and $[(PP_3)Rh(H)Cl]BPh_4$ (**4**) which, by reaction with $NaBH_4$, yield the *cis*-dihydride $[(NP_3)RhH_2]BPh_4$ (**6**) and the monohydride $[(PP_3)RhH]$ (**8**), respectively [$NP_3 = N(CH_2CH_2PPh_2)_3$; $PP_3 = P(CH_2CH_2PPh_2)_3$]. By treatment of **6** in acetone with an excess of $NaBH_4$, the monohydride $[(NP_3)RhH]$ (**7**) is obtained. Protonation of **8** with $HOSO_2CF_3$ followed by addition of $NaBPh_4$ affords the Rh(III) OCT complex $[(PP_3)RhH_2]BPh_4$ (**9**) for which the dichotomy η^2-H_2 versus *cis*-dihydride as a function of temperature has been demonstrated. Metathetical reactions of **2** with organolithium reagents give the σ-organyl complexes $[(PP_3)Rh(CH_3)]$ (**11**) and $[(PP_3)Rh(C_6H_5)]$ (**12**) which react with CO to give the corresponding σ-acyl derivatives $[(PP_3)Rh(COCH_3)]$ (**13**) and $[(PP_3)Rh(COC_6H_5)]$ (**14**). Decoordination of a phosphine arm of PP_3 is a necessary step for the insertion reaction. The monohydride **7** undergoes electrophilic attack by $MeSO_3CF_3$ in THF to give CH_4 and the ortho-metalated hydride $[\{(Ph_2PCH_2CH_2)_2N(CH_2CH_2PPhC_6H_4)\}RhH](SO_3CF_3)$ (**15**) through the intramolecular activation of a phenyl C-H bond. The structure of the iodide derivative $[\{(Ph_2PCH_2CH_2)_2N(CH_2CH_2PPhC_6H_4)\}RhI]BPh_4 \cdot C_6H_6 \cdot 0.5CH_3COCH_3$ (**17a**) was determined by X-ray crystallography. When the methylation of **7** is carried out in THF/benzene mixtures both **15** and the *cis*-(phenyl)hydride $[(NP_3)RhH(C_6H_5)](SO_3CF_3)$ (**22**) are obtained. Decreasing the temperature or increasing the concentration of benzene favors intermolecular C-H activation over cyclometalation. Methylation of **7** in THF followed by addition of an excess of α,α,α-trifluorotoluene gives the *cis*-(trifluorotolyl)hydride $[(NP_3)RhH(C_6H_4CF_3)](SO_3CF_3)$ (**23**) regardless of the temperature. The reductive elimination of the metalated phenyl from **15** is easily promoted by monodentate ligands such as hydride, halides, pseudohalides, pyridine, and CO to form Rh(I) TBP complexes of the formula $[(NP_3)RhX]^{n+}$ ($n = 0, 1$). OCT complexes of rhodium(III), in which the two additional coligands are disposed in mutually cis positions, are obtained by reacting solutions of **15** with a plethora of *addenda* such as H_2, Cl_2, and CS_2. As a result, *cis*-dihydride, *cis*-dichloride, and η^2-CS_2 derivatives are obtained. Dihydrogen elimination from **9**, protonation of **11**, as well as methylation of **8** give $[(PP_3)Rh(SO_3CF_3)]$ (**24**) which exists in two isomeric forms. The $[(PP_3)Rh]^+$ system neither intramolecularly inserts across a C-H bond from a phenyl ring nor intermolecularly activates aromatic C-H bonds. The factors that may be responsible for such a behavior are discussed. Compound **24** reacts with neutral or anionic monodentate ligands affording TBP Rh(I) complexes or oxidatively adds HSO_3CF_3 to give, after addition of $NaBPh_4$, the OCT Rh(III) *cis*-(triflate)hydride $[(PP_3)RhH(SO_3CF_3)]BPh_4$ (**25**).

It is well recognized that $N(CH_2CH_2PPh_2)_3$ (NP_3, I), $P(CH_2CH_2PPh_2)_3$ (PP_3, II), and related tripodal ligands such as $N(CH_2CH_2PCy_2)_3$ (NP_3Cy) can form stable complexes with most d-block metals, although not all of the elements form stable complexes for all of their available oxidation states.[1] Generallay, in fact, these ligands prefer metals in low oxidation states. Rhodium is an exception to the rule: its ability to readily enter into the III → I → III oxidation/reduction cycle does not represent an obstacle to being comfortably coordinated by NP_3[2,3] or PP_3.[1b,c] In most instances, rhodium(I) forms trigonal-bipyramidal (TBP) complexes, which can be attacked by electrophiles to give octahedral (OCT) rhodium(III) derivatives. From the latter, through reductive elimination reactions, the coordinatively and electronically unsaturated systems $[(NP_3)Rh^+]$ and $[(PP_3)Rh^+]$ can form, which either add monofunctional nucleophiles to restore the TBP geometry or oxidatively insert across homo- and heteroatomic bonds to reform OCT Rh(III) complexes.[4,5]

Interesting results in the field of activation of σ-bonds, such as H-H and C-H, by NP_3 and PP_3 complexes of rhodium[4,5] and iridium[6,7] have recently been reported by our group. This prompted us to describe here in detail the synthesis and characterization of several key compounds with which to enter into the fascinating coordination and organometallic chemistry of rhodium complexed to tripodal-tetradentate ligands.

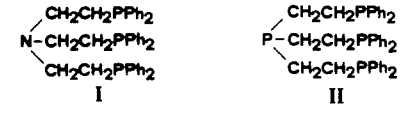

I II

A preliminary communication of part of this work has already appeared.[4]

Experimental Section

All the reactions and manipulations were routinely performed under a nitrogen or argon atmosphere with standard Schlenk techniques. The compounds $[RhCl(COD)]_2$[8] (COD = 1,5-cyclooctadiene), $[(NP_3)RhCl_2]BPh_4$,[2] and $[(NP_3Cy)Rh(H)Cl]BPh_4$[2] and the ligands NP_3[9] and NP_3Cy[10] were prepared according to published procedures. The ligand PP_3 was purchased from Strem Chemicals and used without further purification. Tetrahydrofuran (THF) and diethyl ether were dried over $LiAlH_4$, benzene and aliphatic hydrocarbons over sodium, and di-

(1) (a) Sacconi, L.; Mani, F. *Transition Met. Chem.* **1984**, *8*, 179. (b) King, R. B.; Kapoor, R. N.; Soran, M. S.; Kapoor, P. N. *Inorg. Chem.* **1971**, *10*, 1851. (c) Taqui Khan, M. M.; Martell, A. E. *Ibid.* **1974**, *13*, 2961. (d) Tau, K. D.; Uriarte, R.; Mazanec, T. J.; Meek, D. W. *J. Am. Chem. Soc.* **1979**, *101*, 6614. (e) Puttfarcken, U.; Rehder, D. *J. Organomet. Chem.* **1980**, *185*, 219. (f) Rehder, D.; Oltmann, P.; Hoch, M.; Weidemann, C.; Priebsch, W. *Ibid.* **1986**, *308*, 19. (g) DuBois, D. L.; Miedaner, A. *Inorg. Chem.* **1986**, *25*, 4642. (h) Brüeggeller, P. *Inorg. Chim. Acta* **1987**, *129*, L27.

(2) Di Vaira, M.; Peruzzini, M.; Zanobini, F.; Stoppioni, P. *Inorg. Chim. Acta* **1983**, *69*, 37.

(3) Bianchini, C.; Masi, D.; Mealli, C.; Meli, A.; Sabat, M. *Organometallics* **1985**, *4*, 1014.

(4) Bianchini, C.; Meli, A.; Peruzzini, M.; Zanobini, F. *J. Chem. Soc., Chem. Commun.* **1987**, 971.

(5) Bianchini, C.; Mealli, C.; Peruzzini, M.; Zanobini, F. *J. Am. Chem. Soc.* **1987**, *109*, 5548.

(6) Bianchini, C.; Peruzzini, M.; Zanobini, F. *J. Organomet. Chem.* **1987**, *326*, C29.

(7) Bianchini, C.; Masi, D.; Meli, A.; Peruzzini, M.; Sabat, M.; Zanobini, F. *Organometallics* **1986**, *5*, 2557.

(8) Herde, J. L.; Lambert, J. C.; Senoff, C. V. *Inorg. Synth.* **1974**, *15*, 18.

(9) Morassi, R.; Sacconi, L. *Inorg. Synth.* **1976**, *16*, 174.

(10) Mani, F.; Stoppioni, P. *Inorg. Chim. Acta* **1976**, *16*, 177.

0002-7863/88/1510-6411$01.50/0

chloromethane over P_2O_5. They were purified by distillation under nitrogen just before use. The solid compounds were routinely collected on sintered glass frits and washed, unless otherwise stated, with ethanol and *n*-pentane before being dried in a nitrogen stream. Infrared spectra were recorded on a Perkin-Elmer 283 spectrophotometer with samples mulled in Nujol between KBr plates or dissolved in appropriate solvents. $^{31}P\{^1H\}$ NMR spectra were recorded on VARIAN CFT 20 and VARIAN VXR 300 spectrometers operating at 32.19 and 121.42 MHz, respectively. Peak positions are relative to H_3PO_4 85% with downfield values reported as positive. ^1H NMR spectra were recorded on a VARIAN VXR 300-MHz instrument. Me_4Si was used as an internal reference for all proton spectra. Dihydrogen, methane, and ethylene were detected by GC (Shimadzu) on a Carbosieve S-II column purchased from Supelco. Conductivity measurements were made with a WTW Model LBR/B conductivity bridge.

[(NP$_3$)RhCl] (1). A. Solid NP_3 (1.31 g, 2 mmol) was added to a solution of $[RhCl(COD)]_2$ (0.49 g, 1 mmol) in THF (40 mL). Immediately a purple solution was obtained from which deep purple microcrystals separated. Precipitation was completed by adding ethanol (40 mL). Yield 90%.

B. A solution of $NaBH_4$ (0.08 g, 2 mmol) in ethanol (30 mL) was added portionwise to a solution of $[(NP_3)RhCl_2]BPh_4$ (1.15 g, 1 mmol) in CH_2Cl_2 (30 mL). Immediately a purple solution was obtained from which crystals of **1** separated. Yield 85%. Anal. Calcd for $C_{42}H_{42}ClNP_3Rh$: C, 63.70; H, 5.35; Cl, 4.48; N, 1.77; P, 11.73; Rh, 12.99. Found: C, 63.43; H, 5.47; Cl, 4.22; N, 1.62; P, 11.45; Rh, 12.68.

[(PP$_3$)RhCl] (2). Compound **2** was obtained as a red crystalline solid following the A procedure described above for **1**, using PP_3 instead of NP_3. Yield 90%. Anal. Calcd for $C_{42}H_{42}ClP_4Rh$: C, 62.35; H, 5.23; Cl, 4.38; P, 15.31; Rh, 12.71. Found: C, 62.29; H, 5.11; Cl, 4.17; P, 15.24; Rh, 12.59.

[(NP$_3$)Rh(H)Cl]BPh$_4$ (3). A. To a stirred suspension of **1** (0.79 g, 1 mmol) in THF (70 mL) were added via syringe 100 μL (1.14 mmol) of HSO_3CF_3. The resulting slurry was gently heated to ca. 40 °C for 20–30 min. During this time the starting purple material dissolved to produce a dark green solution. The reaction mixture was allowed to cool to room temperature before solid $NaBPh_4$ (0.50 g, 1.46 mmol) was added. Upon addition of ethanol (50 mL) dark green crystals precipitated. Yield 90%.

B. To a yellow, stirred solution of $[(NP_3)RhCl_2]BPh_4$ (4.45 g, 3 mmol) in acetone (60 mL) was added dropwise an equimolar amount of $NaBH_4$ in ethanol (40 mL). The resulting green solution was evaporated under a stream of nitrogen until **3** began to separate. Addition of *n*-butanol (30 mL) completed the precipitation. Yield 80%. Λ_M (10^{-3} M nitroethane solution) = 57 Ω^{-1} cm^2 mol^{-1}. Anal. Calcd for $C_{66}H_{63}BClNP_3Rh$: C, 71.27; H, 5.71; Cl, 3.19; N, 1.26; P, 8.35. Found: C, 70.98; H, 5.83; Cl, 3.11; N, 1.13; P, 8.20.

[(PP$_3$)Rh(H)Cl]BPh$_4$ (4). To a suspension of **2** (0.81 g, 1 mmol) in THF (60 mL) were added with stirring 100 μL (1.14 mmol) of HSO_3CF_3. Within a few minutes the starting material dissolved to give a pale lilac solution from which lilac needles were obtained after addition of solid $NaBPh_4$ (0.50 g, 1.46 mmol) and ethanol (50 mL). Yield 95%. Λ_M (10^{-3} M nitroethane solution) = 54 Ω^{-1} cm^2 mol^{-1}. Anal. Calcd for $C_{66}H_{63}BClP_4Rh$: C, 70.19; H, 5.62; Cl, 3.14. Found: C, 70.45; H, 6.08; Cl, 3.00.

[(NP$_3$)RhH$_2$]BPh$_4$ (6). A. A solution of $NaBH_4$ (0.15 g, 3.97 mmol) in ethanol (50 mL) was added portionwise to a well-stirred solution of **3** (1.20 g, 1.08 mmol) in THF (100 mL) at room temperature. The temperature was then slowly raised to the boiling point and the reddish solution refluxed for 2 h. Addition of ethanol (100 mL) and concentration of the solution at room temperature under a nitrogen stream gave white crystals of **6**. Yield 65%. Λ_M (10^{-3} M nitroethane solution) = 50 Ω^{-1} cm^2 mol^{-1}. The product was recrystallized from acetone/ethanol.

B. The compound was obtained in 60% yield by refluxing for 3 h a suspension of **3** in ethanol with a 3-fold excess of $NaBH_4$. Anal. Calcd for $C_{66}H_{64}BNP_3Rh$: C, 73.54; H, 5.98; N, 1.30. Found: C, 73.35; H, 6.20; N, 1.19.

[(NP$_3$)RhH] (7). A. Compound **6** (1.10 g, 1.02 mmol) was dissolved in 80 mL of boiling acetone and allowed to react with a large excess of sodium borohydride (0.15 g, 3.97 mmol) in hot ethanol (70 mL). The resulting yellow solution was heated until a large crop of yellow crystals began to separate. Yield 70%.

B. The compound can be synthesized by using LiMe (1.6 M in THF) or LiPh (ca. 2 M in C_6H_6/Et_2O, 75:25) as nucleophilic reagents instead of $NaBH_4$ and dissolving **6** in THF. Yield 50%. Anal. Calcd for $C_{42}H_{43}NP_3Rh$: C, 66.58; H, 5.72; N, 1.85; P, 12.26; Rh, 13.58. Found: C, 66.37; H, 6.03; N, 1.69; P, 12.07; Rh, 13.49.

Reaction of 7 with HSO$_3$CF$_3$ or EtSO$_3$CF$_3$. Addition of neat HSO_3CF_3 (45 μL, 0.5 mmol) or $EtSO_3CF_3$ (55 μL, 0.5 mmol) to a suspension of **7** (0.30 g, 0.4 mmol) in THF (30 mL) caused the solid to dissolve within a few minutes to give a colorless solution. On addition of $NaBPh_4$ (0.27 g, 0.8 mmol) in ethanol (30 mL) white crystals of **6** precipitated in 70% yield.

[(PP$_3$)RhH] (8). To a boiling solution of **4** (1.20 g, 1.06 mmol) in THF (100 mL) was added in small portions a large excess of $NaBH_4$ (0.20 g, 5.29 mmol) in hot ethanol (50 mL). Ethanol (50 mL) was then added to the resulting yellow solution which was concentrated until light yellow microcrystals separated. They were washed with ethanol, distilled water, and ethanol to completely eliminate NaCl. Yield 60%. Anal. Calcd for $C_{42}H_{43}P_4Rh$: C, 65.12; H, 5.60; P, 15.99; Rh, 13.28. Found: C, 64.87; H, 5.83; P, 15.82; Rh, 13.05.

[(PP$_3$)RhH$_2$]BPh$_4$ (9c). Owing to the facile elimination of H_2 from the complex, this reaction was carried out under a H_2 atmosphere to get good yields. Neat HSO_3CF_3 (30 μL, 0.34 mmol) was syringed into a solution of **8** (0.25 g, 0.32 mmol) in THF (10 mL) at 0 °C. The originally yellow solution turned immediately colorless. On addition of $NaBPh_4$ (0.30 g, 0.88 mmol) and ethanol (30 mL) white crystals separated. Yield 90%. Λ_M (10^{-3} M nitroethane solution) = 54 Ω^{-1} cm^2 mol^{-1}. Anal. Calcd for $C_{66}H_{64}BP_4Rh$: C, 72.40; H, 5.89; P, 11.31; Rh, 9.40. Found: C, 72.29; H, 6.03; P, 11.16; Rh, 9.27.

Reaction of 9c with LiHBEt$_3$. $LiHBEt_3$ (1 M in THF, 150 μL, 0.15 mmol) was syringed into a THF solution (10 mL) of **9c** (0.15 g, 0.14 mmol). Yellow microcrystals of **8** were isolated, in 70% yield, after addition of ethanol (15 mL) to the resulting yellow solution.

Reaction of 9c with (PPN)Cl. Addition of (PPN)Cl (0.10 g, 0.17 mmol) to a THF (10 mL) solution of **9c** (0.15 g, 0.14 mmol) gave **2**. Yield 90%.

[(NP$_3$Cy)RhH$_2$]BPh$_4$ (10). Compound **10** was obtained as colorless crystals in an identical fashion to that described for **6**, using $[(NP_3Cy)Rh(H)Cl]BPh_4$ (**5**) instead of **3**. Yield 60%. Λ_M (10^{-3} M nitroethane solution) = 57 Ω^{-1} cm^2 mol^{-1}. Anal. Calcd for $C_{66}H_{100}BNP_3Rh$: C, 67.62; H, 8.60; N, 1.19. Found: C, 67.34; H, 8.83; N, 1.04.

[(PP$_3$)Rh(CH$_3$)] (11). LiMe (1.6 M in THF, 0.6 mL, 0.96 mmol) was added to a suspension of **2** (0.50 g, 0.62 mmol) in THF (70 mL). The resulting slurry was stirred for 3 h. During this time the starting material dissolved to give a yellow solution. Addition of ethanol and slow evaporation of the solvent gave yellow microcrystals. Yield 55%. Anal. Calcd for $C_{43}H_{45}P_4Rh$: C, 65.48; H, 5.75. Found: C, 63.34; H, 5.71.

[(PP$_3$)Rh(C$_6$H$_5$)] (12). This yellow complex was prepared as described for **11** except for substitution of LiPh (ca. 2 M in C_6H_6/Et_2O, 75:25, 0.50 mL, 1.0 mmol) for LiMe. Yield 60%. Anal. Calcd for $C_{48}H_{47}P_4Rh$: C, 67.77; H, 5.56. Found: C, 67.54; H, 5.53.

[(PP$_3$)Rh(COCH$_3$)] (13). Carbon monoxide was bubbled for 20 min throughout a THF (20 mL) suspension of **11** (0.30 g, 0.88 mmol) until a lemon yellow solution was obtained. Addition of ethanol (20 mL) and concentration in a fast stream of nitrogen gave lemon yellow crystals. Yield 75%. Anal. Calcd for $C_{44}H_{45}OP_4Rh$: C, 64.71; H, 5.55; Rh, 12.60. Found: C, 64.04; H, 5.61; Rh, 12.43.

[PP$_3$Rh(COC$_6$H$_5$)] (14). Yellow crystals of the benzoyl derivative were prepared from the phenyl derivative **12** with the method used for **13**. Yield 70%. Anal. Calcd for $C_{49}H_{47}OP_4Rh$: C, 66.97; H, 5.39; Rh, 11.71. Found: C, 66.84; H, 5.31; Rh, 11.53.

[{(Ph$_2$PCH$_2$CH$_2$)$_2$N(CH$_2$CH$_2$PPhC$_6$H$_4$)}RhH](SO$_3$CF$_3$) (15). A suspension of **7** (0.30 g, 0.40 mmol) in THF (15 mL) was treated with a slight excess of $MeSO_3CF_3$ (60 μL, 0.54 mmol) at 0 °C under magnetic stirring. In a few minutes the starting yellow solid dissolved while the color gradually disappeared (occasionally clear pink). Addition of two volumes of *n*-heptane caused the precipitation of **15** as a microcrystalline white solid, which was collected by filtration and washed with *n*-pentane. Yield 90%. Anal. Calcd for $C_{43}H_{42}F_3NO_3P_3RhS$: C, 57.02; H, 4.67; N, 1.55; P, 10.26; Rh, 11.36. Found: C, 56.49; H, 4.85; N, 1.35; P, 10.14; Rh, 11.28.

[{(Ph$_2$PCH$_2$CH$_2$)$_2$N(CH$_2$CH$_2$PPhC$_6$H$_4$)}RhCl]BPh$_4$ (16). Addition of 3 equiv of chloroform to a colorless solution of **15** (prepared as above) caused an immediate color change to pale green. On addition of solid $NaBPh_4$ (0.30 mg, 0.88 mmol) and ethanol (20 mL), followed by slow evaporation of the solvent, green crystals were obtained. Yield 85%. Λ_M (10^{-3} M nitroethane solution) = 53 Ω^{-1} cm^2 mol^{-1}. Anal. Calcd for $C_{66}H_{61}BClNP_3Rh$: C, 71.40; H, 5.54; N, 1.26; Cl, 3.19. Found: C, 71.27; H, 5.73; N, 1.12; Cl, 3.01.

[{(Ph$_2$PCH$_2$CH$_2$)$_2$N(CH$_2$CH$_2$PPhC$_6$H$_4$)}RhI]BPh$_4$ (17). The orange ortho-metalated iodo derivative was prepared by the above procedure with iodoform as halogenating reagent. Crystals of $[\{(Ph_2PCH_2CH_2)_2N(CH_2CH_2PPhC_6H_4)\}RhI]BPh_4 \cdot C_6H_6 \cdot 0.5CH_3COCH_3$ (**17a**) were obtained by recrystallization from a dilute acetone–benzene (3:1) solution. Yield 90%. Λ_M (10^{-3} M nitroethane solution) = 50 Ω^{-1} cm^2 mol^{-1}. Anal. Calcd for $C_{73.5}H_{70}BINO_{0.5}P_3Rh$: C, 67.45; H, 5.39; N, 1.07; I, 9.69. Found: C, 67.30; H, 5.52; N, 0.91; I, 9.38.

[(NP$_3$)RhI] (18). A solution of **15** (0.20 g, 0.22 mmol) in THF (20 mL) was treated with LiI (0.04 g, 0.28 mmol). There was an immediate color change from colorless to deep red and, in a few minutes, precipitation of dark red crystals occurred. Yield 95%. Anal. Calcd for $C_{42}H_{42}INP_3Rh$: C, 57.10; H, 4.79; I, 14.36; N, 1.58; Rh, 11.65. Found: C, 56.81; H, 4.99; I, 13.93; N, 1.46; Rh, 11.53.

[(NP$_3$)RhN$_3$] (19). Purple microcrystals of compound **19** were obtained through the procedure used to synthesize **18** replacing LiI with (PPN)N$_3$. Yield 90%. Anal. Calcd for $C_{42}H_{42}N_4P_3Rh$: C, 63.16; H, 5.30; N, 7.01. Found: C, 62.84; H, 5.53; N, 6.89.

Reaction of 15 with (PPN)Cl. Solid (PPN)Cl (0.20 g, 0.35 mmol) was added to a solution of **15** (0.30 g, 0.33 mmol) in THF (30 mL). Immediately the solution turned purple and separated microcrystals of **1**. Yield 80%.

Reaction of 15 with CS$_2$. Carbon disulfide vapors were bubbled through a THF (10 mL) solution of **15** (0.20 g, 0.22 mmol). The color became immediately orange. Addition of solid NaBPh$_4$ (0.20 g, 0.60 mmol) and ethanol (10 mL) gave orange microcrystals of [(NP$_3$)Rh(CS$_2$)]BPh$_4$ (**29**). Yield 85%.

Reaction of 15 with Cl$_2$. A slow stream of chlorine was bubbled in a THF (10 mL) solution of **15** (0.20 g, 0.22 mmol) at 0 °C for 5 min, in which time the solution became yellow. On addition of NaBPh$_4$ (0.30 g, 0.88 mmol) and ethanol (10 mL) [(NP$_3$)RhCl$_2$]BPh$_4$ separated as yellow crystals. Yield 75%.

[(NP$_3$)Rh(CO)]BPh$_4$ (20). A. Carbon monoxide was bubbled for 15 min into a THF (20 mL) solution of **15** (0.20 g, 0.22 mmol) to give a yellow solution. Addition of solid NaBPh$_4$ (0.30 g, 0.88 mmol) and ethanol (20 mL), followed by slow concentration of the resulting solution, gave yellow-green crystals. Yield 70%.

B. Analogously this compound was obtained by bubbling carbon monoxide through a THF (30 mL) solution of **6** (1.10 g, 1 mmol) and working up as above. Yield 65%. Λ_M (10^{-3} M nitroethane solution) = 59 Ω^{-1} cm^2 mol^{-1}. Anal. Calcd for $C_{67}H_{62}BNOP_3Rh$: C, 72.90; H, 5.66; N, 1.27; P, 8.42. Found: C, 72.85; H, 5.87; N, 1.17; P, 8.26.

Reaction of 15 with H$_2$. Dihydrogen was bubbled for 20 min through a THF (20 mL) solution of **15** (0.20 g, 0.22 mmol). Addition of NaBPh$_4$ (0.30 g, 0.88 mmol) and ethanol (20 mL) to the colorless solution gave **6**. Yield 65%.

Reaction of 15 with LiHBEt$_3$. LiHBEt$_3$ (1 M in THF, 150 μL, 0.15 mmol) was syringed into a THF solution (10 mL) of **15** (0.12 g, 0.13 mmol). Addition of ethanol (15 mL) and concentration of the solution yielded **7**. Yield 75%.

[(NP$_3$)Rh(NC$_5$H$_5$)]BPh$_4$ (21). Neat pyridine (1.0 mL, 12.43 mmol) was pipetted into a THF solution (20 mL) of **15** (0.30 g, 0.33 mmol). Immediately the solution became deep red and separated dark red crystals after addition of solid NaBPh$_4$ (0.30 mg, 0.88 mmol) and ethanol (20 mL). Yield 90%. Λ_M (10^{-3} M nitroethane solution) = 57 Ω^{-1} cm^2 mol^{-1}. Anal. Calcd for $C_{72}H_{67}BN_2P_3Rh$: C, 74.10; H, 5.79; N, 2.40; P, 7.96; Rh, 8.82. Found: C, 74.12; H, 5.87; N, 2.36; P, 7.76; Rh, 8.58.

[(NP$_3$)RhH(C$_6$H$_5$)](SO$_3$CF$_3$) (22). A suspension of **7** (0.30 g, 0.40 mmol) in a THF–benzene (2:1) mixture (30 mL) was treated with a slight excess of MeSO$_3$CF$_3$ (60 μL, 0.54 mmol) at 0 °C. The starting material dissolves in a few minutes to give a clear solution. Addition of 50 mL of *n*-heptane precipitated a microcrystalline white solid, which was filtered off and washed with *n*-pentane. Yield 85%. Anal. Calcd for $C_{49}H_{48}F_3NO_3P_3RhS$: C, 59.82; H, 4.92; N, 1.42; Rh, 10.46. Found: C, 59.73; H, 4.99; N, 1.39; Rh, 10.32.

[(NP$_3$)RhH(C$_6$H$_4$CF$_3$)](SO$_3$CF$_3$) (23). To a suspension of **7** (0.30 g, 0.40 mmol) in THF (20 mL) at 0 °C were added 0.5 mL (4.11 mmol) of α,α,α-trifluorotoluene and then 65 μL (0.59 mmol) of neat MeSO$_3$CF$_3$. The solution became pale yellow in a few minutes. Addition of *n*-heptane (40 mL) precipitated white microcrystals, which were filtered off and washed with *n*-pentane. Yield 75%. Anal. Calcd for $C_{50}H_{47}F_6NO_3P_3RhS$: C, 57.10; H, 4.50; N, 1.33. Found: C, 57.22; H, 4.67; N, 1.27.

[(PP$_3$)Rh(SO$_3$CF$_3$)] (24). A. To a solution of **8** (0.40 g, 0.52 mmol) in benzene (50 mL), neat MeSO$_3$CF$_3$ (65 μL, 0.59 mmol) was added. The initial yellow color immediately disappeared to produce a deep purple solution from which purple crystals began to separate with a few minutes. The solid was washed twice with benzene and *n*-pentane. Yield 90%.

B. To a well-stirred suspension of **11** (0.30 g, 0.38 mmol) in benzene (40 mL) was added dropwise a solution of HSO$_3$CF$_3$ (35 μL, 0.40 mmol) in THF (5 mL). Microcrystals of **24** formed as soon as the reactant was added. Yield 85%. Anal. Calcd for $C_{43}H_{42}F_3O_3P_4RhS$: C, 55.98; H, 4.59; P, 13.43; Rh, 11.15; S, 3.47. Found: C, 55.57; H, 4.62; P, 13.23; Rh, 11.02; S, 3.29.

Reaction of 24 with H$_2$. A solution of **8** (0.20 g, 0.26 mmol) in THF (10 mL) was treated with a slight excess of MeSO$_3$CF$_3$ (30 μL, 0.27 mmol). The reaction mixture immediately turned red. Dihydrogen was slowly bubbled through the solution causing a rapid fading of the color. Addition of NaBPh$_4$ (0.30 g, 0.88 mmol) and ethanol (10 mL) gave colorless crystals of **9**. Yield 80%.

Reaction of 24 with HSO$_3$CF$_3$. A large excess of triflic acid (88 μL, 1.00 mmol) was syringed into a solution of **24** in 10 mL of THF prepared as described above. As soon as the acid was added, the solution became colorless. Addition of 15 mL of ethanol containing 0.50 g (1.46 mmol) of NaBPh$_4$ precipitated white crystals of [(PP$_3$)RhH(OSO$_2$CF$_3$)BPh$_4$ (**25**). Yield 70%. Anal. Calcd for $C_{67}H_{63}BF_3P_4RhS$: C, 64.75; H, 5.11. Found: C, 64.32; H, 5.23.

[(PP$_3$)RhN$_3$] (26). Compound **26** was synthesized as orange crystals by the same procedure used for **19**, using a solution of **24** instead of one of **15**. Yield 90%. Anal. Calcd for $C_{42}H_{42}N_3P_4Rh$: C, 61.85; H, 5.19; N, 5.15; Rh, 12.62. Found: C, 61.84; H, 5.30; N, 5.03; Rh, 12.50.

Reaction of 24 with (PPN)Cl. Analogously to the reaction of **15** with (PPN)Cl, the reaction of **24** with this salt gave the chloride **2** in 75% yield.

[(PP$_3$)Rh(CO)]BPh$_4$ (27). A. The carbonyl derivative **27** was synthesized as described for the NP$_3$ analogue, using **24** instead of **15**.

B. Carbon monoxide was bubbled for 30 min into a THF (10 mL) solution of **9** (0.15 g, 0.14 mmol) at room temperature. Addition of ethanol (15 mL) and slow concentration of the pale yellow solution under nitrogen gave **27**. Yield 85%. Λ_M (10^{-3} M nitroethane solution) = 52 Ω^{-1} cm^2 mol^{-1}. Anal. Calcd for $C_{67}H_{62}BOP_4Rh$: C, 79.06; H, 6.14. Found: C, 78.93; H, 6.37.

Reaction of 24 with LiHBEt$_3$. Compound **8** was obtained in 80% yield by reacting **24** with LiHBEt$_3$ as described for the NP$_3$ analogue.

[(PP$_3$)Rh(PPh$_3$)]BPh$_4$ (28). Solid triphenylphosphine (0.25 g, 0.95 mmol) was added to a THF solution (20 mL) of **24** (0.60 g, 0.65 mmol). Addition of NaBPh$_4$ (0.30 g, 0.88 mmol) and ethanol (25 mL) gave canary yellow crystals. Yield 90%. Λ_M (10^{-3} M nitroethane solution) = 50 Ω^{-1} cm^2 mol^{-1}. Anal. Calcd for $C_{84}H_{77}BP_5Rh$: C, 74.45; H, 5.73; P, 11.43; Rh, 7.73. Found: C, 74.20; H, 5.78; P, 11.32; Rh, 7.36.

X-ray Data Collection and Structure Determination. A summary of crystal and intensity data is presented in Table V. All X-ray measurements were performed on a Philips PW 1100 automated, four-circle diffractometer with a Mo Kα radiation monochromatized with a graphite crystal. A set of 25 reflections were carefully centered to determine the unit cell. As a general procedure, three standard reflections were collected every 2 h (no decay of intensities was observed in any case). The data were corrected for Lorentz and polarization effects. The transmission factors ranged between 0.99 and 0.95. Atomic scattering factors were those tabulated by Cromer and Waber[11] with anomalous dispersion corrections taken from ref 12. The computational work was essentially performed with the SHELX76 system.[13] The structure was solved by the Patterson and Fourier techniques. Refinement was done by full-matrix least-squares calculations initially with isotropic thermal parameters. Anisotropic thermal parameters were used only for the I, Rh, and P atoms. The phenyl rings, with the exception of the ortho-metalated one, were treated as rigid bodies of D_{6h} symmetry with C–C distances fixed at 1.395 Å and calculated hydrogen atom positions (C–H, 1.0 Å). A difference map showed some relatively high peaks which were attributed to benzene and acetone solvent molecules. From elemental and spectroscopic analysis the stoichiometric ratio between the complex and the solvent molecules is 1:1:0.5. Since the thermal parameters relative to benzene and acetone refine to acceptable values by assuming atomic population parameters of 1 and 0.5, respectively, the ratio given above is confirmed to be correct. The final difference Fourier map has the largest peaks of 1.06 and 1.01 e/Å^3 which appear to be iodine and rhodium ripples, respectively. Final coordinates of all the non-hydrogen atoms are reported in Table VI.

Results and Discussion

The preparations and the principal reactions of the complexes described in this paper are reported in Schemes I–III.

The straightforward reaction of [RhCl(COD)]$_2$ with the tripodal polyphosphines NP$_3$ and PP$_3$ in dry THF is an excellent method for the synthesis of [(NP$_3$)RhCl] (**1**) and [(PP$_3$)RhCl] (**2**), two key starting materials for the chemistry of rhodium with NP$_3$ and PP$_3$. Alternatively, **1** can be prepared by treatment of the dichloride [(NP$_3$)RhCl$_2$]BPh$_4$ in CH$_2$Cl$_2$ with 2 equiv of NaBH$_4$ in ethanol.[2] It is, however, more convenient to use the former route as it provides higher yields based on hydrated rho-

(11) Cromer, D. T.; Waber, J. T. *Acta Crystallogr.* **1965**, *18*, 104.
(12) *International Tables of Crystallography*; Kynoch: Birmingham, England, 1974; Vol. 4.
(13) Sheldrick, G. M. SHELLX76 Program for Crystal Structure Determinations; University of Cambridge: Cambridge, England, 1976.

Scheme I

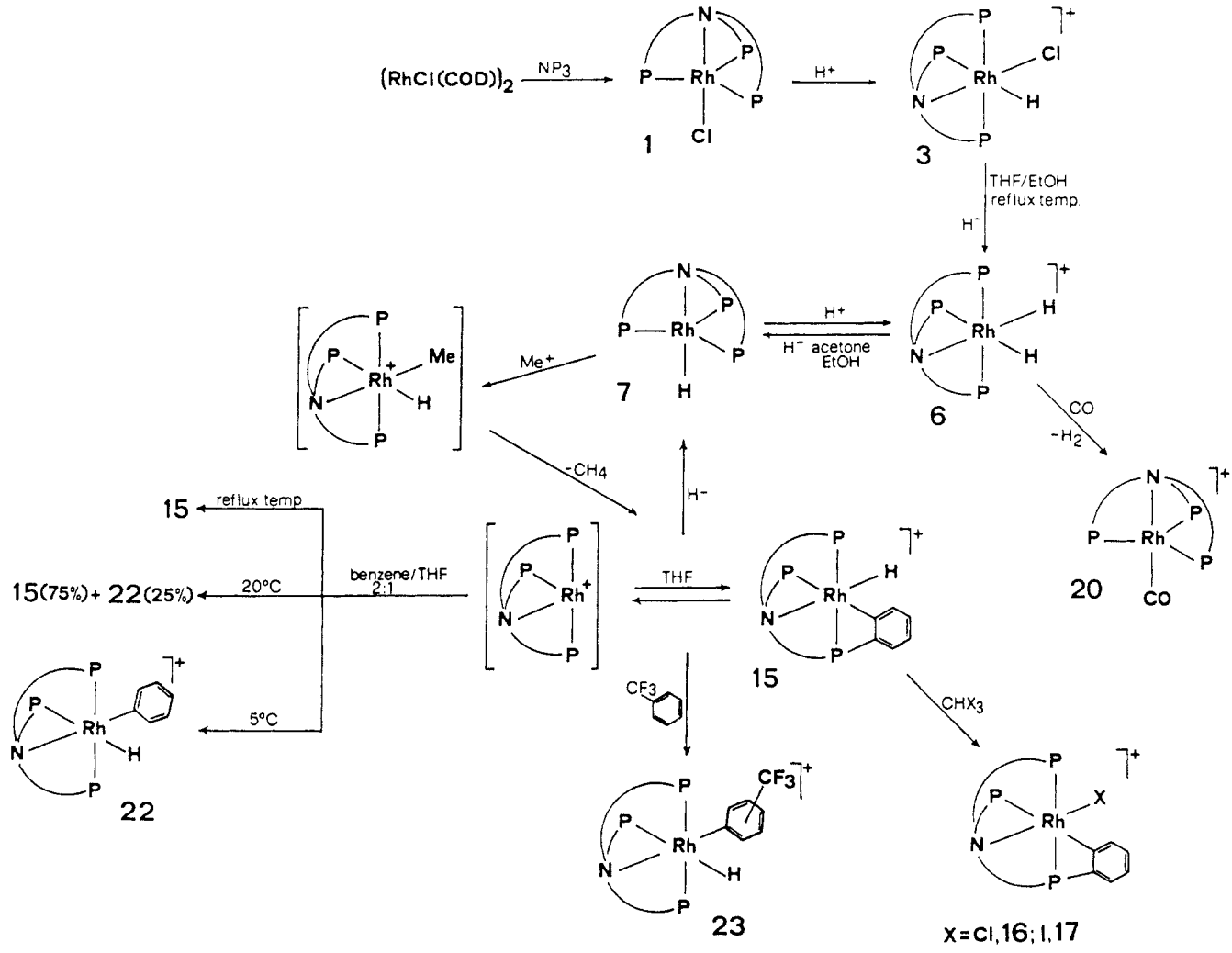

Scheme II

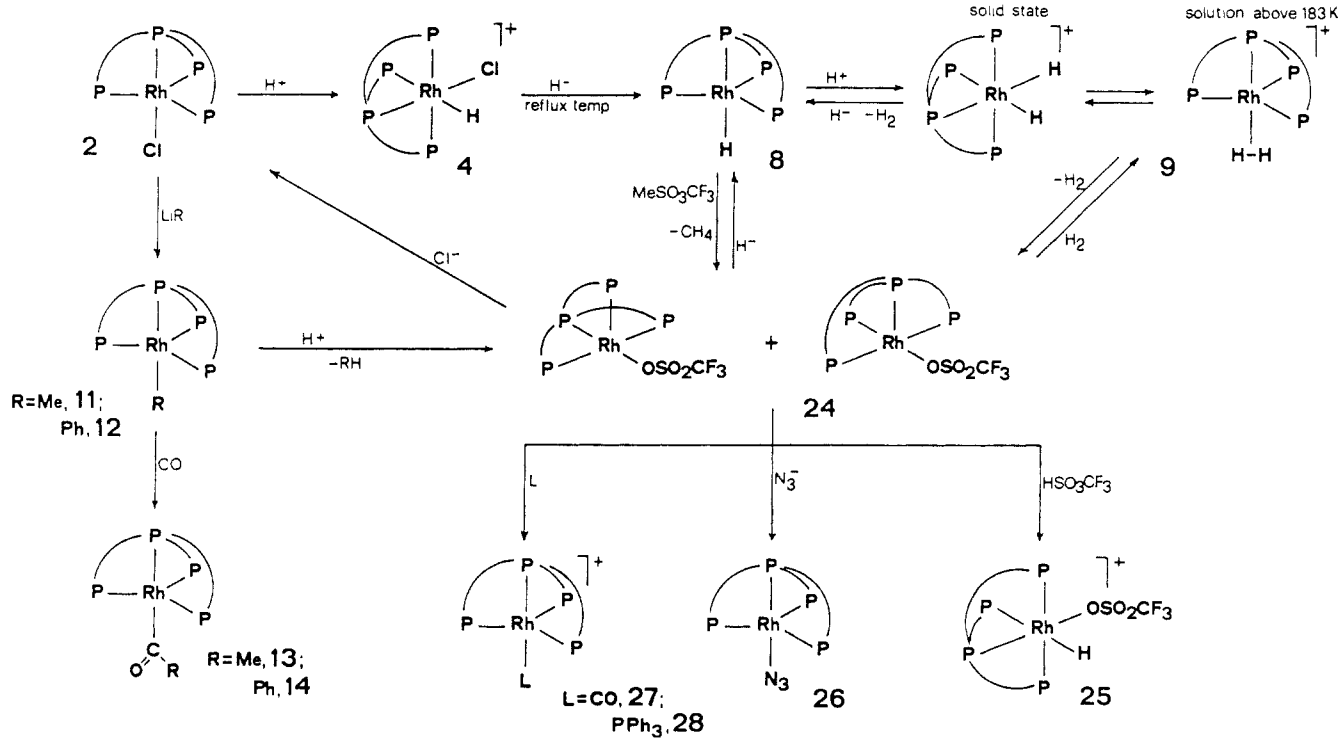

Table I. $^{31}P\{^1H\}$ NMR Data for the Rh(I) Pentacoordinate Complexes

compound	chemical shifts[a,b] $\delta(P_A)$	$\delta(P_M)$	coupling constant, Hz $J(PP)$	$J(P_ARh)$	$J(P_MRh)$	coord chemical shifts[c] $\Delta(P_A)$	$\Delta(P_M)$
$[(PP_3)RhCl]$ (**2**)	146.18	39.68	17.1	127.5	147.3	160.33	58.58
$[(NP_3)RhH]$[d] (**7**)		39.59			174.9		58.71
$[(PP_3)RhH]$[d] (**8**)	158.88	63.99	19.2	88.5	162.0	173.03	82.89
$[(PP_3)Rh(CH_3)]$ (**11**)	153.22	46.38	17.9	88.7	161.4	167.37	65.28
$[(PP_3)Rh(Ph)]$ (**12**)	145.25	46.60	18.2	81.1	160.8	159.40	65.50
$[(PP_3)Rh(COCH_3)]$ (**13**)	136.35	44.39	20.7	77.4	170.3	150.50	63.29
$[(PP_3)Rh(COPh)]$ (**14**)	136.23	44.14	21.8	77.0	167.3	150.38	63.04
$[(NP_3)Rh(CO)]BPh_4$ (**20**)		39.55			134.1		58.67
$[(NP_3Rh(py)]BPh_4$ (**21**)		22.29			153.9		41.41
$[(PP_3)RhN_3]$ (**26**)	142.37	42.81	17.9	118.9	148.2	156.52	61.71
$[(PP_3)Rh(CO)]BPh_4$ (**27**)	151.39	60.54	24.9	83.8	132.9	165.54	79.44
$[(PP_3)Rh(PPh_3)]BPh_4$[e] (**28**)	142.29	42.97	22.9	91.1	140.1	156.44	61.87

[a] Chemical shifts (δ) are relative to 85% H_3PO_4, with positive values being downfield from the standard. The spectra were recorded in CH_2Cl_2 solutions at room temperature, unless otherwise stated. [b] P_A is the designation for the bridgehead phosphorus atom of the PP_3 ligand; P_M is the designation for the PPh_2 peripheral groups of both PP_3 and NP_3. [c] Free ligands: PP_3, $\delta(P_A) = -14.15$, $\delta(P_M) = -18.90$, $J(PP) = 24.0$ Hz. NP_3, $\delta(P_M) = -19.12$. [d] Acetone solution. [e] $\delta(PPh_3) = 27.44$, $J(P_APPh_3) = 279.1$, $J(P_MPPh_3) = 40.1$, $J(RhPPh_3) = 100.7$.

Scheme III

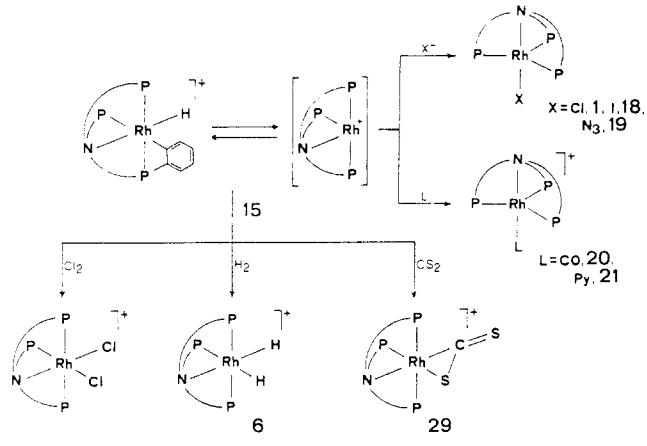

dium trichloride which is the rhodium source shared by both procedures.

Compounds **1** and **2** are air-stable in the solid state and in deoxygenated solutions. The solubility of **1** was so low as to preclude a meaningful characterization in solution. By contrast, **2** is fairly soluble in halogenated solvents. The $^{31}P\{^1H\}$ NMR spectrum in CH_2Cl_2 consists of a simple first-order AM_3X splitting pattern that produces a quartet for the central bridgehead phosphorus atom and a doublet for the three terminal P atoms of the PP_3 ligand (Table I). The latter resonance is shifted upfield with respect to that of the apical phosphorus atom of the tripodal ligand. Obviously, each resonance is doubled by coupling with the ^{103}Rh nucleus. The ^{31}P NMR spectrum is quite consistent with a TBP structure (IV), in which the chloride and the bridgehead phosphorus atom lie trans to each other in axial positions. Such a structure is exhibited also in the solid state as the compound is isomorphous (X-ray powder diagram) with the isoelectronic TBP $[(PP_3)CoH]$ derivative which was authenticated by an X-ray analysis.[14] This geometry can be extended to the NP_3 derivative **1** (III) which, in turn, is isomorphous with the TBP Co(I) hydride $[(NP_3)CoH]$.[15] Interestingly, the analogous Co(I) complex $[(NP_3)CoCl]$ is paramagnetic with a magnetic moment corresponding to two unpaired spins and possesses a distorted tetrahedral geometry, the nitrogen atom being uncoordinated.[16] According to theoretical calculations of the extended Hückel type, it was stressed that the σ-donor capabilities of the ligand trans to the amine ultimately determine whether diamagnetic TBP or high-spin pseudotetrahedral complexes are formed.[16] AOM calculations for a TBP $[(NP_3)RhX]$ chromophore (X = monodentate ligand) have shown that for a e_σ^N/e_σ^X ratio >1, and this occurs for X = Cl, the ground state is a singlet in nice agreement with the diamagnetism of **1**.

Compound **2** (suspended in THF) readily undergoes straightforward metathetical reactions with main group organometallic compounds. Thus, the alkyl and aryl derivatives $[(PP_3)RhR]$ [R = CH_3 (**11**); C_6H_5 (**12**)] are obtained as yellow crystals. By contrast, the chloride **1** does not react with LiMe or LiPh even under drastic reaction conditions, most likely as a result of changing the apical donor atom from phosphorus to nitrogen, the former lying much higher in the *trans* influence series.

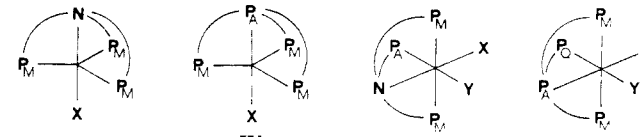

Both compounds **11** and **12** are air-stable in the solid state and in deoxygenated acetone, THF, halogenated hydrocarbons, and nitroethane solutions. The IR spectra do not provide much information, the only significant absorbance being exhibited by **12** at 1560 cm^{-1}, which is due to an additional ν(C–C) phenyl vibration. The $^{31}P\{^1H\}$ NMR spectra exhibit typical AM_3X spin systems that permit one to assign both compounds a TBP geometry in solution (IV).

Compounds **11** and **12** (suspended in THF) readily react with carbon monoxide at atmospheric pressure and room temperature to give lemon yellow crystalline acetyl and benzoyl derivatives of formulas $[(PP_3)Rh(COCH_3)]$ (**13**) and $[(PP_3)Rh(COC_6H_5)]$ (**14**). Both compounds are air-stable in the solid state and in deoxygenated solutions and the insertion of CO is a nonreversible process. The presence of acyl ligands is evidenced by IR spectra which show strong C=O stretching vibrations at 1575 and 1540 cm^{-1} for **13** and **14**, respectively.[17] The $^{31}P\{^1H\}$ NMR spectra exhibit AM_3X patterns and are consistent with TBP geometries for both compounds (IV). As a pedagogic example of the spectral patterns observed for this family of TBP $[(PP_3)RhX]$ complexes, the spectrum of the methyl derivative **11** is shown in Figure 1a. The coupling constants and the chemical shifts for all of the compounds are listed in Table I.

The ^1H NMR spectra of the methyl and acetyl derivatives in the aliphatic proton region contain unresolved multiplets (3 H), which are not present in the spectra of the starting chloride (Table II). The resonance at 0.38 ppm in the spectrum of **11** is assigned

(14) Ghilardi, C. A.; Sacconi, L. *Cryst. Struct. Commun.* **1975**, *4*, 149.
(15) Sacconi, L.; Ghilardi, C. A.; Mealli, C.; Zanobini, F. *Inorg. Chem.* **1975**, *14*, 1380.
(16) Ghilardi, C. A.; Mealli, C.; Midollini, S.; Orlandini, A. *Inorg. Chem.* **1985**, *24*, 164.
(17) (a) McCooey, K. M.; Probitts, E. J.; Mawby, R. J. *J. Chem. Soc., Dalton Trans.* **1987**, 1713. (b) Walker, J. A.; Zheng, L.; Knober, C. B.; Soto, J.; Hawthorne, M. F. *Inorg. Chem.* **1987**, *26*, 1608. (c) Jabloski, C. R. *Ibid.* **1981**, *20*, 3940.

Table II. ^1H NMR Data for the Complexes[a]

compound	chemical shift[b]	coupling constants, Hz
$[(NP_3)Rh(H)Cl]BPh_4$ (**3**)	δ(RhH) = −7.80 dq	$J(P_A)$ = 192.2; $J(P_M)$ = J(Rh) = 6.8
$[(PP_3)Rh(H)Cl]BPh_4$ (**4**)	δ(RhH) = −8.51 ds	$J(P_Q)$ = 172.4; $J(P_M)$ = 18.5; $J(P_A)$ = J(Rh) = 9.0
$[(NP_3)RhH_2]BPh_4$ (**6**)	δ(RhH) = −8.86 dm, −14.42 m	$J(P_A)$ = 137.7
$[(NP_3)RhH]$[c] (**7**)	δ(RhH) = −17.90 dq	$J(P_M)$ = J(Rh) = 24.2
$[(PP_3)RhH]$[c] (**8**)	δ(RhH) = −6.56 dq	$J(P_A)$ = 130.0; $J(P_M)$ = J(Rh) = 17.0
$[(PP_3)RhH_2]BPh_4$[d] (**9**)	δ(RhH) = −5.10 dm, −10.15 dm	$J(P_A)$ = 135.0 $J(P_M)$ = 130.0
$[(NP_3Cy)RhH_2]BPh_4$ (**10**)	δ(RhH) = −11.56 dm, −16.50 m	$J(P_A)$ = 118.0
$[(PP_3)Rh(CH_3)]$ (**11**)	$\delta(CH_3)$ = 0.38 b	
$[(PP_3)Rh(COCH_3)]$ (**13**)	$\delta(COCH_3)$ = 2.16 b	
$[\{(Ph_2PCH_2CH_2)_2N(CH_2CH_2PPhC_6H_4)\}RhH]SO_3CF_3$[c] (**15**)	δ(RhH) = −11.50 m	
$[(NP_3)RhH(C_6H_5)]SO_3CF_3$[c] (**22**)	δ(RhH) = −8.10 dm	$J(P_A)$ = 130.0
$[(NP_3)RhH(C_6H_4CF_3)]SO_3CF_3$[c] (**23**)	δ(RhH) = −11.30 dm	$J(P_M)$ = 125.0
$[(PP_3)RhH(SO_3CF_3)]BPh_4$[c] (**25**)	δ(RhH) = −7.43 ds	$J(P_M)$ = 133.5; $J(P_M)$ = 17.8; $J(P_A)$ = J(Rh) = 8.5

[a] All ^1H NMR spectra were recorded at 300 MHz at room temperature in CD_2Cl_2 solutions unless otherwise stated. [b] In ppm from external TMS. The resonance due to hydrogen atoms belonging to the NP_3, NP_3Cy, and PP_3 ligands are not reported; key: b = broad; d = doublet, q = pseudoquintuplet, s = pseudosextet, m = multiplet. [c] In CD_3COCD_3 solution. [d] In C_4D_8O solution at 173 K. Over 183 K the pattern rearranges to a doublet of pseudoquintuplet centered at −7.39 ppm, $J(HP_{trans})$ = 67.0 Hz, $J(HP_{cis})$ = J(HRh) = 13.7 Hz, see text and ref 5.

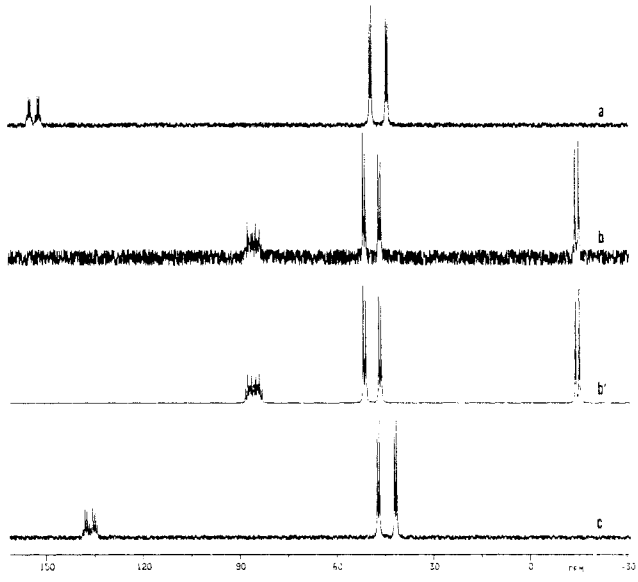

Figure 1. $^{31}P\{^1H\}$ NMR (CH_2Cl_2, 213 K, 32.19 MHz) of $[(PP_3)Rh(CH_3)]$ (a), $[(Ph_2PCH_2CH_2)P(CH_2CH_2PPh_2)_2Rh(CO)(CH_3)]$ (b, experimental spectrum; b', computed spectrum), and $[(PP_3)Rh(COCH_3)]$ (c). H_3PO_4 reference.

to the methyl ligand[17b,18] while the similar but low-field resonance at 2.16 ppm in the spectrum of **13** is assigned to the methyl group on the acetyl ligand.[17b] This signal is partially superimposed to the $-CH_2-$ resonance of the polyphosphine ethylenic chains. In both cases, very small couplings with the phosphorus and rhodium nuclei are observed [J(HP) ≃ J(HRh) < 2 Hz].

The carbonyl insertion reaction[19,20] is a key step in many homogeneous catalytic processes.[21] Theoretical[22] and experimental[23] studies of CO insertions in five-coordinate d^8 systems agree in describing the reactions as alkyl migrations via four-coordinate acyl intermediates. On steric and electronic grounds, a mechanism of this type can be extended to the present $[(PP_3)RhR]$ systems provided that unfastening of a terminal phosphine of PP_3 to allow

Scheme IV

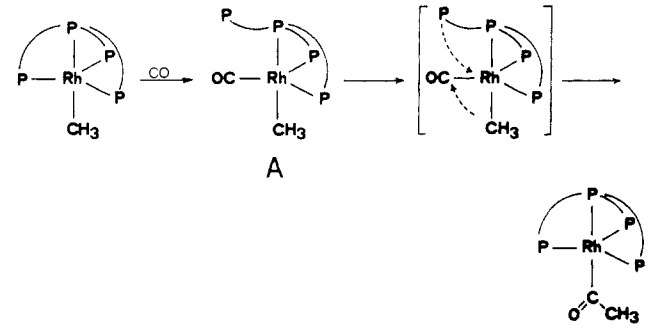

CO to enter the coordination sphere of rhodium occurs. Indeed, we have been able to spectroscopically detect the occurrence of an intermediate complex containing a coordinated carbonyl ligand and a dangling phosphine arm of PP_3 in the course of the formal CO insertion into the Rh–C bond of **11** (Scheme IV). The carbonyl group in intermediate A has deliberately been located in an equatorial site because of the better back-bonding in that position.[24,25]

The $^{31}P\{^1H\}$ NMR spectrum at −60 °C of a CH_2Cl_2 solution of **11** saturated with CO clearly shows the presence of a free phosphine arm, P_Q, which resonates at −14.89 ppm [$J(P_QP_A)$ = 37.81 Hz]. The overall spin system is of the AM_2QX type with δP_A = 85.43 ppm [$J(P_AP_M)$ = 22.95 Hz, $J(P_ARh)$ = 77.2 Hz] and δP_M = 48.70 ppm [$J(P_MRh)$ = 154.65 Hz] (Figure 1b) in nice agreement with that previously reported by Meek et al. for the complex $[(PP_3)Rh(NO)]$ which exhibits a free phosphine donor.[26] Elimination of the excess of CO from the CH_2Cl_2 solution by bubbling nitrogen into the NMR tube leads to the quantitative formation of the acyl complex **13**, as evidenced by the appearance of its typical ^{31}P NMR AM_3X pattern (Figure 1c). Evidence for the presence of a coordinated carbonyl ligand in intermediate A is provided by the IR spectrum of the CH_2Cl_2 solution of **11** saturated with CO which shows a strong absorption at 1920 cm^{-1}. Remarkably, both the position and the intensity of this band are very similar to those observed for the carbonyl ligand in the strictly related five-coordinate complex $[(triphos)Rh(CO)(CH_3)]$.[27]

We have reacted the homoleptic σ-organyl complexes $[(PP_3)CoR]$[28] and $[(PP_3)IrR]$[6] (R = CH_3, C_6H_5) with CO (1 atm,

(18) Lilga, M. A.; Sohn, Y. S.; Ibers, J. A. *Organometallics* **1986**, *5*, 766.
(19) Calderazzo, F. *Angew. Chem., Int. Ed. Engl.* **1977**, *16*, 299.
(20) Wojcicki, A. *Adv. Organomet. Chem.* **1973**, *11*, 83.
(21) (a) Pruett, R. L. *Adv. Organomet. Chem.* **1979**, *17*, 1. (b) Forster, D. *Ibid.* **1979**, *17*, 255. (c) Masters, C. *Ibid.* **1979**, *17*, 61. (d) Bradley, J. S. *Ibid.* **1979**, *101*, 7419.
(22) Berke, H.; Hoffmann, R. *J. Am. Chem. Soc.* **1978**, *100*, 7224.
(23) (a) Heck, R. F. *Acc. Chem. Res.* **1969**, *2*, 10. (b) Piacenti, F.; Bianchi, M.; Benedetti, E. *Chem. Ind. (Milan)* **1967**, *49*, 245. (c) Nagy-Magos, Z.; Bor, G.; Markó, L. *J. Organomet. Chem.* **1968**, *14*, 205.
(24) Rossi, A. R.; Hoffmann, R. *Inorg. Chem.* **1975**, *14*, 365.
(25) Dahlenburg, L.; Mirzaei, F. *Inorg. Chim. Acta* **1985**, *97*, L1.
(26) Mazanek, T. J.; Tau, K. D.; Meek, D. W. *Inorg. Chem.* **1980**, *19*, 85.
(27) Johnston, G. G.; Baird, M. C. *J. Organomet. Chem.* **1986**, *314*, C51.
(28) Stoppioni, P.; Dapporto, P.; Sacconi, L. *Inorg. Chem.* **1978**, *17*, 718.

Table III. $^{31}P\{^1H\}$ NMR Data for the Octahedral Rh(III) Complexes

compound		chemical shift[a] $\delta(P_A)$	$\delta(P_M)$	$\delta(P_Q)$	coupling constants, Hz $J(P_AP_M)$	$J(P_AP_Q)$	$J(P_MP_Q)$	$J(P_ARh)$	$J(P_MRh)$	$J(P_QRh)$
$\|(NP_3)Rh(H)Cl\|BPh_4$ (**3**)	AM_2X	11.63	34.18		20.0			84.9	102.9	
$\|(PP_3)Rh(H)Cl\|BPh_4$ (**4**)	AM_2QX	138.99	43.95	31.45	7.0	4.4	17.9	96.7	87.6	112.7
$\|(NP_3)RhH_2\|BPh_4$ (**6**)	AM_2X	47.97	37.13		21.00			113.2	99.0	
$\|(PP_3)RhH_2\|BF_4$[b] (**9**)	AM_2QX	139.79	62.70	59.30	<2	2.5	10.2	69.6	75.0	70.3
$\|(NP_3Cy)RhH_2\|BPh_4$ (**10**)	AM_2X	54.14	41.80		16.2			97.3	104.5	
$\|\{(Ph_2PCH_2CH_2)_2N(CH_2CH_2PPhC_6H_4)\}RhH\|SO_3CF_3$ (**15**)	AMQX	25.70	12.95	−34.08	22.6	436.1	13.2	104.3	80.9	74.8
$\|\{(Ph_2PCH_2CH_2)_2N(CH_2CH_2PPhC_6H_4)\}RhCl\|BPh_4$ (**16**)	AMQX	24.25	11.24	−35.64	23.1	436.9	13.8	103.8	80.9	75.3
$\|(NP_3)RhH(C_6H_5)\|SO_3CF_3$ (**22**)	AM_2X	23.64	31.97		21.9			115.7	91.5	
$\|(NP_3)RhH(C_6H_4CF_3)\|SO_3CF_3$ (**23**)	AM_2X	34.28	47.80		26.3			98.4	123.7	
$\|(PP_3)Rh(OSO_2CF_3)\|$ (**24**)	AM_2QX a	112.33	52.06	24.70	26.9	14.2	34.3	119.7	140.9	132.1
	b	104.15	52.06	16.52						
$\|(PP_3)RhH(OSO_2CF_3)\|BPh_4$ (**25**)	AM_2QX	133.58	47.73	34.39	4.0	5.0	17.2	109.7	97.6	84.3

[a] The chemical shifts (δ) are relative to 85% H_3PO_4, with positive values being downfield from the standard. The spectra were recorded in acetone solutions at room temperature (298 K). [b] In TDF solution at 173 K. The pattern rearranges to an AM_3X one over 183 K (see text and ref 5). At 298 K, in TDF solution: $\delta(P_A)$ = 140.14, $\delta(P_M)$ = 60.78, $J(P_AP_M)$ = 5.7 Hz, $J(P_ARh)$ = 71.0 Hz, $J(P_MRh)$ = 101.1 Hz.

298 K). In no case was CO insertion observed. While the behavior of the iridium complexes is not unexpected because of the stronger metal–carbon bonds (recall that the strength of the M–C bonds increases down the triad M = Co, Rh, Ir),[29] the stability of the cobalt complexes with respect to CO insertion is not so easily interpretable. Certainly, an important role in determining the chemistry of the cobalt complexes is played by the lesser basicity of cobalt versus rhodium. This fact may make it more difficult to replace a phosphine by the less donating CO group and, therefore, may impede the CO insertion through an intermediate of type A.

Reaction of **1**, suspended in THF, with $HOSO_2CF_3$ under vigorous stirring gives the Rh(III) complex $[(NP_3)Rh(H)Cl]BPh_4$ (**3**), isolated as green crystals following addition of solid $NaBPh_4$ and absolute ethanol.

The ease with which TBP complexes of rhodium(I) are attacked by electrophiles at the metal is a result of the capability of these systems to arrange an occupied frontier σ orbital upon slight displacement of one ligand in the equatorial plane of the trigonal-bipyramid.[30] Alternatively, the cis-(hydride)chloride **3** is synthesized by reaction of the dichloride $[(NP_3)RhCl_2]BPh_4$ in acetone with 1 equiv of $NaBH_4$ in ethanol. The solutions of the latter two coreactants must be mixed very slowly to prevent formation of the Rh(I) chloride **1**.

Complex **3** is air-stable both in the solid state and in solution. It is soluble in halogenated hydrocarbons, nitroethane, acetone, and THF, in which it behaves as a 1:1 electrolyte. The IR spectrum of the green crystals reveals a characteristic band at 2000 cm^{-1}, assigned to the ν(Rh–H) vibration. The presence of the BPh_4^- anion was confirmed both by the typical band located at ca. 610 cm^{-1} and by a reinforced phenyl vibration at 1580 cm^{-1}. Interestingly, **3** is converted to a yellow isomer by exposure to visible light. These two compounds are spectroscopically indistinguishable in solution (IR, NMR) so that the difference in color is attributed to a solid-state effect. As a matter of fact, the IR spectrum of the yellow isomer mulled in Nujol exhibits ν(Rh–H) at a lower wave number (1960 cm^{-1}). A similar significant shift of the metal–hydrogen stretching vibration (65 cm^{-1}) was found for two isomers of the hydride $[(NP_3)CoH]$ whose structures differ only in phenyl ring conformation.[31] Observation of analogous light sensitivity for a Fe(II) dihydride with diphos, $Ph_2PCH_2CH_2PPh_2$, has been previously reported.[32]

The $^{31}P\{^1H\}$ NMR spectrum (Table III) exhibits a typical first-order AM_2X pattern consistent with an octahedral geometry in which the hydride and chloride ligands occupy cis positions of the coordination sphere (V). The resonance for the mutually trans phosphorus atoms of the tripodal ligand, P_M, appears as a doublet of doublets due to coupling with rhodium and the residual phosphorus atom, P_A. The signal of the latter nucleus appears as a doublet of triplets. This pattern arises from coupling with the two mutually trans phosphorus atoms, P_M, and rhodium.

In the ^1H NMR spectrum (Table II) the resonances assigned to the CH_2 and aromatic protons of the NP_3 ligand are located in the expected regions while a hydridic resonance appears in the high-field region of the spectrum. The signal, centered at −7.80 ppm, consists of two well-separated quartets. This pattern arises from coupling with the trans phosphorus atom P_A, [$^2J(HP_{trans})$ = 192.9 Hz], with the two equivalent phosphorus atoms, P_M, and rhodium [$^2J(HP_{cis}) \simeq {}^1J(HRh)$ = 6.8 Hz]; the coincidence of the latter coupling constants to give pseudomultiplets has been previously observed for several phosphine complexes.[33]

Like the NP_3 analogue, compound **2** reacts with triflic acid to give lilac needles of $[(PP_3)Rh(H)Cl]BPh_4$ (**4**) after metathetical reaction with $NaBPh_4$ in ethanol. Elemental analysis, conductivity, and spectroscopic data are fully consistent with a monocationic complex having OCT geometry (VI). The $^{31}P\{^1H\}$ NMR spectrum presents a first-order AM_2QX spin system with three well-separated signals of relative intensities 1:2:1 (Table III). The high-frequency resonance, assigned to P_A, appears as a doublet of triplets of doublets originated by coupling with rhodium, and the two equivalent P_M atoms. In turn, each component of the two triplets is doubled by coupling with the remaining terminal phosphorus atom, P_Q. The most intense resonance, located at 43.95 ppm, is assigned to the two phosphorus atoms P_M lying trans to each other and consists of a doublet of doublets of doublets, due to coupling with rhodium, the central phosphorus atom, P_A, and the terminal phosphorus nucleus, P_Q. Once again, the resonance of the latter phosphorus atom, which invariably is the most upfield in the present series of PP_3 octahedral rhodium complexes, appears as a doublet of triplets of doublets owing to coupling with rhodium, the two mutually trans P_M atoms, and the central P_A nucleus. The chemical shifts and coupling constants are in the range found for other Rh(III) complexes with mono- and polydentate phosphines.[34] As expected, the resonances of the PP_3 phosphorus atoms are highly downfield with respect to the free ligand. These high values of the coordination chemical shifts, Δ [$\Delta = \delta(P_{coord}) - \delta(P_{free\ ligand})$] are principally due to the ring contribution as each phosphorus donor is bound in a five-membered metallorings.[35] A noticeable feature is represented by the coupling constants between the two types of terminal phosphorus atoms, which are larger than those involving the central P donor, i.e., $J(P_MP_Q) \gg J(P_AP_M) \simeq J$-

(29) Ziegler, T.; Tschinke, V.; Becke, A. *J. Am. Chem. Soc.* **1987**, *109*, 1351 and references therein.
(30) Bianchini, C.; Meli, A.; Dapporto, P.; Tofanari, A.; Zanello, P. *Inorg. Chem.* **1987**, *26*, 3677.
(31) Stoppioni, P.; Dapporto, P. *Cryst. Struct. Commun.* **1979**, *8*, 15.
(32) Ittel, S. D.; Tolman, C. A.; Krusic, P. J.; English, A. D.; Jesson, J. P. *Inorg. Chem.* **1978**, *17*, 3432.
(33) Slack, D. A.; Greveling, I.; Baird, M. C. *J. Am. Chem. Soc.* **1979**, *101*, 3125.
(34) Pregosin, P. S.; Kunz, R. W. *^{31}P and ^{13}C NMR of Transition Metal Phosphine Complexes*; Diehl, P., Fluck, E., Kosfeld, R., Eds.; Springer-Verlag: Berlin-Heidelberg-New York, 1979.
(35) Garrou, P. E. *Chem. Rev.* **1981**, *81*, 229.

(P_AP_Q). This phenomenon has been previously observed and attributed to coupling through the carbon backbone of the ligand which reduces the coupling occurring through the metal.[36]

While in **3** the position of the hydride ligand in the coordination sphere is unequivocally assigned on the basis of NMR experiments (the H atom lies trans to a phosphorus atom rather than to nitrogen), in the PP_3 analogue **4**, the ^1H NMR spectrum does not permit one to determine the position occupied by the hydride ligand in the coordination polyhedron. In other words, it is not possible to deduce whether the hydride ligand is trans either to P_A or to P_Q. This uncertainty has been solved by recording a ^{31}P NMR spectrum without proton decoupling. Such a spectrum shows that while the downfield signal is only broadened by coupling with the methylenic and aromatic protons of the ligand, the upfield one is resolved into two distinct broad signals. The large coupling constant between these signals, whose value closely approaches that found in the proton spectrum of **4**, permits the location of the hydride ligands trans to one of the terminal PPh_2 substituents of the polyphosphane, namely P_Q (see VI). This result is confirmed by the X-ray structure of the closely related Ru(II) complex $[\{P(CH_2CH_2CH_2PMe_2)_3\}Ru(H)Cl]$[37] as well as by other ^{31}P NMR data of metal complexes with tripodal polyphosphane ligands having a P_4 donor atom set.[38]

Regardless of the solvent, the reaction of $[RhCl(COD)]_2$ with NP_3Cy affords no isolable product. The same phenomenon is observed also for the NP_3Et ligand [NP_3Et = $N(CH_2CH_2PEt_2)_3$].[39] These two tetradentate ligands differ in the size of the alkyl substituents on the phosphorus atoms. We therefore conclude that the presence of aryl substituents plays a critical role in stabilizing TBP Rh(I) complexes with tripodal tetradentate ligands. As far as we have been able to ascertain, the only entry to rhodium chemistry with NP_3Cy is the one previously indicated by one of us, i.e., the straightforward reaction of NP_3Cy with $RhCl_3$ hydrate in ethanol.[2] In this way, $[(NP_3Cy)RhCl_2]Cl$ is obtained, which is converted to the OCT hydride $[(NP_3Cy)Rh(H)Cl]BPh_4$ (**5**) by treatment with an excess of $NaBPh_4$ in CH_2Cl_2/ethanol. The crystal structure of **5**, determined by X-ray methods,[2] showed that the hydride ligand is located trans to a phosphorus donor, in nice agreement with our findings for **3** and **4**.

The *cis*-(hydride)chloride complexes $[LRh(H)Cl]BPh_4$ [L = NP_3 (**3**); NP_3Cy (**5**)] react in THF solution or suspended in ethanol with an excess of $NaBH_4$ to give the dihydride complexes $[LRh(H)_2]BPh_4$ (L = NP_3 (**6**); NP_3Cy (**10**)). Both compounds are air-stable in the solid state and in acetone, THF, and nitroethane solutions in which they behave as 1:1 electrolytes. The IR spectra exhibit strong bands at 2000 (**6**) and 2025 cm^{-1} (**10**) which are assigned to ν(Rh–H). The $^{31}P\{^1H\}$ NMR spectra exhibit AM_2X patterns and are consistent with octahedral geometries in which the two hydride ligands are located in the equatorial plane trans to the P_A phosphorus atom and the bridgehead nitrogen. In accordance with such a geometry, the proton NMR spectra show three unresolved multiplets in the hydride region with relative intensities 0.5:0.5:1. The two downfield resonances constitute a doublet originated by the hydride ligand trans to the equatorial phosphorus P_A [$J(HP_A)$ = 137.7 Hz for **6** and 118.0 Hz for **10**]. Consequently, the high-field signal is attributed to the hydride trans to nitrogen. Interestingly, when the reaction of **3** with ethanolic $NaBH_4$ is carried out in acetone, the solution becomes immediately dark red and quickly separates a crop of red microcrystals of **1**, which occasionally contains traces of the hydride **6**. Unlike the PP_3 analogue $[(PP_3)RhH_2]^+$, for which the dichotomy η^2-H_2 (TBP) versus *cis*-dihydride (OCT) as a function of temperature has been demonstrated (see below),[5] **6** maintains the classical *cis*-dihydride structure also in ambient temperature solutions. As a matter of fact, the monodeuteriated $[(NP_3)Rh(H)D]^+$ complex cation, obtained by electrophilic attack on the TBP monohydride $[(NP_3)RhH]$ (**7**) by CF_3CO_2D in THF, exhibits a J(HD) coupling constant of ca. 2 Hz, which rules out any bonding between the *cis*-hydride and deuteride ligands.[5] Also, **6** shows two distinct T_1 parameters (THF, 298 K) for the hydride ligands with values of 450 and 600 ms, thus indicating absence of H–H interaction.[40] However, H–H bonding can be easily promoted by externally added ligands such as CO to give the TBP Rh(I) carbonyl $[(NP_3)Rh(CO)]BPh_4$ (**20**) and H_2. In nice agreement with the low propensity to form five-coordinate Rh(I) complexes, the NP_3Cy derivative **10** does not eliminate H_2 on reaction with CO.

Scheme V

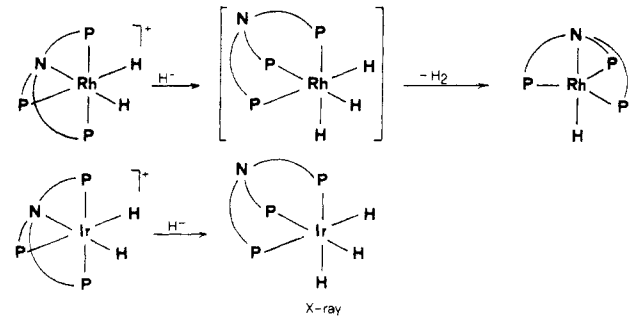

The *cis*-(dihydride) **6** reacts with organolithium reagents such as LiMe or LiPh to yield, following the reductive elimination of CH_4 or C_6H_6, respectively, the TBP hydride $[(NP_3)RhH]$ (**7**). However, the best method to prepare **7** is the addition of an excess of $NaBH_4$ in ethanol to the dihydride **6** dissolved in boiling acetone. In the course of the reaction, H_2 is evolved. Although we have not been able to detect any intermediate complex, we propose the pathway shown in Scheme V to explain the formation of **7**. This involves the intermediacy of a trihydride of rhodium(III) in which NP_3 behaves as a tridentate ligand. As the amine reenters the coordination sphere of the metal, H_2 is reductively eliminated and the monohydride forms. Such a mechanism finds support in the isolation and X-ray characterization of the trihydride $[(NP_3)IrH_3]$ obtained by reacting $[(NP_3)Ir(H)_2]^+$ with $LiAlH_4$ under the same conditions used for the rhodium reaction.[41] The stability of the Ir(III) trihydride with respect to dihydrogen elimination is likely a consequence of both the remarkable strength of the Ir–H bond as well as the major kinetic inertness of iridium compounds as compared to rhodium.[42]

Compound **7** is a yellow crystalline material, sparingly soluble in THF and acetone and insoluble in alcohols, hydrocarbons, and diethyl ether. Halogenated solvents cause the immediate precipitation of **1** through metathetical reaction. The compound quickly decomposes when exposed to air or moisture. Its IR spectrum is characterized by the presence of a strong sharp band at 1935 cm^{-1}, which is due to the stretching vibration of the Rh–H bond. The $^{31}P\{^1H\}$ NMR spectrum (Table I) consists of a single resonance at 39.59 ppm doubled by the large coupling with the ^{103}Rh nucleus [J(PRh) = 174.9 Hz]. The ^1H NMR spectrum in the high-field region shows a well-resolved pseudoquintuplet arising from the fortuitous coincidence of J(HP) and J(HRh). Related systems (quartets) have been observed for the isoelectronic complexes $[(NP_3)CoH]$[15] and $[(NP_3)NiH]BPh_4$[43] for which X-ray diffraction analyses established TBP structures. While the resonance of the hydride ligand in **7** is only relatively low-field shifted with respect to those of the cobalt and nickel analogues [δH_{Rh} = –17.9 ppm, δH_{Co} = –25.9 ppm, δH_{Ni} = –23.2 ppm], it is worth noticing that the J(HP) coupling constants involving the first-row transition metals are much higher [$^2J(H_MP)$ = 12.7 Hz (M =

(36) Hohman, W. H.; Kountz, D. J.; Meek, D. W. *Inorg. Chem.* **1986**, *25*, 616.
(37) Antberg, M.; Dahlenburg, L. *Acta Crystallogr.* **1986**, *C42*, 997.
(38) Dawson, J. W.; Venanzi, L. *J. Am. Chem. Soc.* **1968**, *90*, 7229.
(39) Bianchini, C.; Mealli, C.; Meli, A.; Sacconi, L. *Inorg. Chim. Acta* **1980**, *43*, 223.
(40) Crabtree, R. H.; Lavin, M.; Bonneviot, L. *J. Am. Chem. Soc.* **1986**, *108*, 4032.
(41) Bianchini, C.; Mealli, C.; Peruzzini, M.; Vizza, F.; Zanobini, F. *J. Organomet. Chem.* **1988**, *346*, C53.
(42) (a) Buchanan, J. M.; Stryker, J. M.; Bergman, R. G. *J. Am. Chem. Soc.* **1986**, *108*, 1537. (b) Crabtree, R. H. *Chem. Rev.* **1985**, *85*, 245.
(43) Sacconi, L.; Orlandini, A.; Midollini, S. *Inorg. Chem.* **1974**, *13*, 2850.

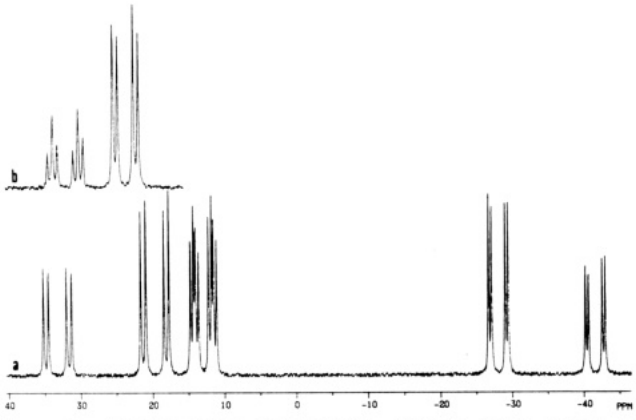

Figure 2. $^{31}P\{^1H\}$ NMR (CH_3COCH_3, 298 K, 32.19 MHz) of $[\{(Ph_2PCH_2CH_2)_2N(CH_2CH_2PPhC_6H_4)\}RhH](SO_3CF_3)$ (a) and $[(N\text{-}P_3)RhH(C_6H_5)](SO_3CF_3)$ (b). H_3PO_4 reference.

Scheme VI

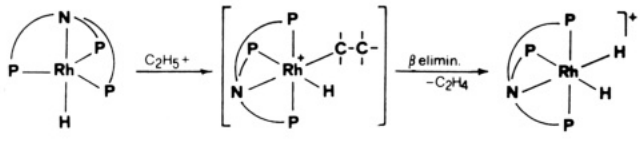

Rh), 50.5 Hz (M = Co), and 37.5 Hz (M = Ni)].

On the basis of all of these data it is therefore reasonable to assign a TBP structure to **7** where the nitrogen and the hydrogen atoms lie trans to each other in axial positions. The coordination of the amine group is shown by the IR spectrum which does not contain the diagnostic band at 2800 cm^{-1} exhibited whenever the nitrogen apical atom of the NP_3 ligand is uncoordinated.[44]

Compound **7** in THF solution is highly reactive toward a great variety of electrophilic reagents. The dihydride **6** can be easily reobtained by reacting **7** with strong acids or with the ethyl cation from $EtOSO_2CF_3$. The latter reaction reasonably proceeds via a β-elimination process from an octahedral *cis*-(hydride)ethyl intermediate (the formation of C_2H_4 was determined by GC) (Scheme VI).[45]

When the electrophilic attack on **7** in THF is carried out with Me^+ from $MeOSO_2CF_3$, methane is evolved. The formation of methane is most likely due to a reductive elimination reaction from an unstable *cis*-(methyl)hydride of Rh(III) that so far we have not been able to detect. The 16-electron fragment $[(NP_3)Rh]^+$ that forms is not isolable since it readily inserts across an ortho C–H bond from one of the six phenyl substituents on the phosphorus atoms and the ortho-metalated hydride $[\{(Ph_2PCH_2CH_2)_2N(CH_2CH_2PPhC_6H_4)\}RhH](SO_3CF_3)$ (**15**) precipitates by addition of *n*-heptane to the reaction mixture (Scheme I).

The ortho-metalated structure of **15** is strongly supported by the IR spectrum which exhibits an additional phenyl vibration at 1580 cm^{-1} and ν(Rh–H) at 2000 cm^{-1}.[46] The $^{31}P\{^1H\}$ NMR spectrum (Figure 2a), showing an AMQX pattern, is consistent with an octahedral geometry around rhodium. In particular, one of the P–P coupling constants, namely $^2J(P_AP_Q)$, has the value of 436.1 Hz in nice agreement with the presence of two different phosphorus atoms lying trans to each other, one of which engaged in a four-membered metallorings.[35] The presence of a phosphorus atom of the latter type is indicated by the high-field resonance at −34.08 ppm. The ^1H NMR spectrum exhibits a high-field signal whose multiplicity is not well resolved even at low temperature. On the other hand, the absence of any strong halving of the signal permits one to locate the hydride ligand trans to nitrogen. This is an interesting result since in the *cis*-(hydride)chloride derivatives

(44) Bianchini, C.; Meli, A.; Scapacci, G. *Organometallics* **1985**, *2*, 1834.
(45) Doherty, N. M.; Bercaw, J. E. *J. Am. Chem. Soc.* **1985**, *107*, 2670.
(46) Bennet, M. A.; Milner, D. L. *J. Am. Chem. Soc.* **1969**, *91*, 6983.

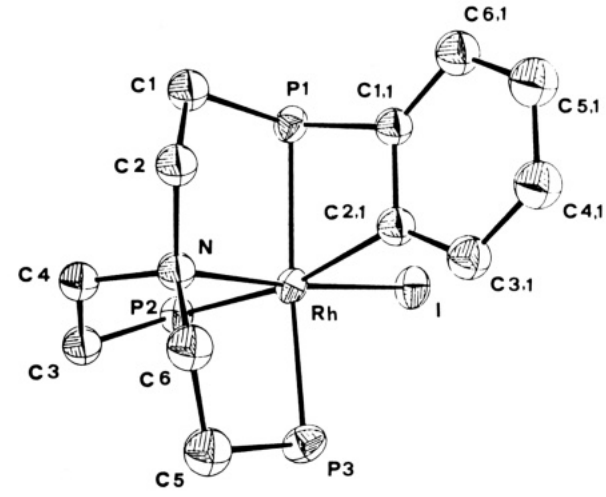

Figure 3. ORTEP drawing and labeling scheme for **17a**.

Table IV. Selected Bond Lengths (Å) and Angles (deg) for **17a**

Rh–I	2.655 (1)	I–Rh–P1	91.50 (1)
Rh–P1	2.325 (2)	I–Rh–P2	94.42 (1)
Rh–P2	2.356 (3)	I–Rh–P3	99.21 (1)
Rh–P3	2.321 (2)	I–Rh–N	175.03 (2)
Rh–N	2.156 (7)	I–Rh–C2,1	88.94 (2)
Rh–C2,1	2.12 (1)	N–Rh–C2,1	90.46 (3)
P1–C1	1.816 (9)	Rh–P1–C1,1	85.88 (3)
P1–C1,1	1.79 (1)	Rh–C2,1–C1,1	105.60 (6)
P2–C3	1.84 (1)	Rh–C2,1–C3,1	138.83 (7)
P3–C5	1.84 (1)	Rh–P1–C1	102.23 (3)
N–C2	1.53 (1)	P1–C1,1–C6,1	133.88 (7)
N–C4	1.51 (1)	P2–Rh–C2,1	168.10 (2)
N–C6	1.49 (1)	P2–Rh–N	85.21 (2)
C1–C2	1.49 (1)	P2–Rh–P3	94.30 (1)
C3–C4	1.50 (1)	P3–Rh–C2,1	96.44 (2)
C5–C6	1.49 (1)	P3–Rh–N	85.76 (2)
C1,1–C2,1	1.39 (1)	P1–Rh–C2,1	67.00 (3)
C1,1–C6,1	1.38 (2)	P1–C1,1–C2,1	100.6 (6)
C2,1–C3,1	1.39 (1)		
C5,1–C6,1	1.38 (2)		
C3,1–C4,1	1.37 (2)		
C4,1–C5,1	1.35 (1)		

3–5 as well as all the known octahedral monohydride metal complexes of NP_3, NP_3Cy, and PP_3, the hydride ligand is invariably located cis to the bridgehead donor atom of the tripodal ligand (vide infra). The reasons for this unique feature must be likely sought in the steric requirements associated with the intramolecular C–H bond activation.

Compound **15** is fairly stable in the solid state and in deoxygenated solutions but decomposes to intractable material when exposed to air. Conversely, it can be greatly stabilized by metathesizing the hydride ligand with halides. This can be done by treating THF solutions of **15** with an excess of halogenated hydrocarbons such as $CHCl_3$ and CHI_3. In such a way, after the addition of $NaBPh_4$, pale green and orange crystals of $[\{(Ph_2PCH_2CH_2)_2N(CH_2CH_2PPhC_6H_4)\}RhCl]BPh_4$ (**16**) and $[\{(Ph_2PCH_2CH_2)_2N(CH_2CH_2PPhC_6H_4)\}RhI]BPh_4$ (**17**) are obtained. Compounds **16** and **17** are much easier to handle than their hydridic precursors since both are air-stable both in the solid state and in solution. The crystal structure of $\mathbf{17}\cdot C_6H_6\cdot 0.5CH_3COCH_3$ (**17a**) has been determined by X-ray methods. The ORTEP drawing of the complex cation is shown in Figure 3.

Selected bond angles and distances are reported in Table IV. The structure consists of discrete mononuclear $[\{(Ph_2PCH_2CH_2)_2N(CH_2CH_2PPhC_6H_4)\}RhI]^+$ cations, BPh_4^- anions, and solvate benzene and acetone molecules in the stoichiometric ratio of 1:0.5. In nice agreement with the chemical–physical characterization of the complex, the metal is in a distorted OCT environment being coordinated by the four donor atoms of NP_3, an iodide ligand, and an ortho carbon atom from one of the NP_3 phenyl rings. As expected, the iodine atom lies

trans to nitrogen. The Rh–I bond length of 2.655 (1) Å well matches those found for other rhodium(III) phosphine complexes containing iodide ligands.[47] The ortho-metalated benzene ring is slightly deformed in the endocyclic angles at C(11), C(21), and C(61). The former angle, which involves the carbon atom of the phenyl ring bonded to P(1), widens by ca. 5° while the other two, located in ortho positions with respect to C(11), are consistently narrowed by ca. 4° [C(21) is the carbon atom directly bonded to rhodium]. The remaining endocyclic angles as well as the C–C bond distances do not present significant variations. Overall, the benzene ring retains its planarity [$\Sigma(\Delta/\sigma)^2 = 3.7$]. The internal angles of the rhodaphosphacyclobutane ring [C(21)–Rh–P(1), Rh–P(1)–C(11), and C(11)–C(21)–Rh are 67.00 (3), 85.88 (3), and 105.60 (6)°, respectively] are much smaller than the idealized values of 90°, 120°, and 109°. Such a distortion of the four-membered cyclometalated ring clearly indicates considerable ring strain. Finally, the rhodaphosphacyclobutane ring shows a very small deviation from planarity, the dihedral angle RhP(1)C(21)–C(11)P(1)C(21) being 5.4 (4)°. As previously reported, this reduced puckering appears as a constant feature of ortho-metalated complexes whatever the metal involved in the ring system.[48]

Interestingly, the intramolecular C–H bond activation affording **15** can be reversed to formally restore the 16-electron fragment $[(NP_3)Rh]^+$ either thermally or by addition of suitable substrates. In particular, when the electrophilic attack by Me^+ on **7** is carried out in a 2:1 mixture of THF/benzene at reflux temperature, the only product obtained is **15**. On decreasing the temperature, the insertion of the 16-electron $[(NP_3)Rh]^+$ system across a C–H bond from benzene begins to occur concurrently with the intramolecular ortho-metalation reaction. At 20 °C, **15** and the *cis*-(hydride)-phenyl complex $[(NP_3)RhH(C_6H_5)](SO_3CF_3)$ (**22**) are formed in a ratio of 3:1. At 5 °C, only the activation of benzene takes place to give **22** in almost quantitative yield (Scheme I). The composition of the equilibrium mixture at any stage of the reaction can be monitored by IR, ^1H, and $^{31}P\{^1H\}$ NMR spectroscopies. The latter method is particularly useful to follow the course of the reaction as the AM_2X splitting pattern of **22** is easily distinguishable from the AMQX one of **15** (Figure 2b).

Despite the fact that several metal complexes capable of both intramolecularly (cyclometalation) and intermolecularly activating C–H bonds have appeared in the literature,[49] a clear-cut explanation of the factors which control these relative reactivities has been offered for a few cases only.[49c,d] It has been pointed out that steric crowding is responsible for propensity of some systems to cyclometalate. As in our case, Bergman and Wenzel[49b] found that decreasing the temperature favors intermolecular C–H activation over cyclometalation. We now add that the concentration of the organic substrate bearing the C–H bond tips the balance in favor of the intermolecular reaction. In particular, we have found that for benzene/THF molecular ratios below 0.1, only the ortho-metalated hydride forms regardless of the temperature. By contrast, increasing the ratio while keeping the temperature fixed increases the amount of the *cis*-(phenyl)hydride **22**.

Another factor that strongly favors intermolecular C–H bond activation over cyclometalation is the introduction of electron-withdrawing substituents on benzene. As an example, α,α,α-trifluorotoluene, whose C–H bonds are certainly activated by the trifluoromethyl substituent, reacts at room temperature with the ortho-metalated hydride **15** in THF solution to give quantitatively the *cis*-(hydride)trifluorotolyl complex $[(NP_3)RhH(C_6H_4CF_3)](SO_3CF_3)$ (**23**). However, a 10-fold excess of the arene is necessary to depress completely cyclometalation. As previously reported, both ortho and para C–H bonds of $C_6H_5CF_3$ can be cleaved by metal systems.[50] Unfortunately, crowding in the aromatic proton region due to the presence of the six phenyl groups of NP_3 did not permit us to discriminate between the two possible isomers by ^1H NMR techniques.

Scheme VII

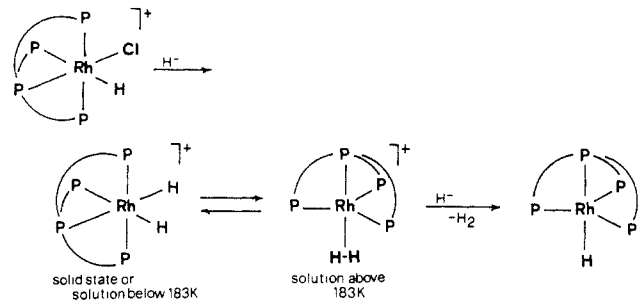

The aryl hydrides **22** and **23** are colorless microcrystalline materials that can be stored at room temperature for days without apparent decomposition. Their IR spectra contain medium intensity bands at 2010 and 1580 cm^{-1} assigned to ν(Rh–H) and ν(C–C) of the σ-aryl ligands, respectively. Moreover, **23** exhibits a strong IR band at 1430 cm^{-1}, which is indicative of the trifluoromethyl group.[51] ^1H and $^{31}P\{^1H\}$ NMR measurements (Tables II and III) are consistent with the OCT structural formulation given in Scheme I.

Considering the ease with which the 16-electron $[(NP_3)Rh]^+$ fragment inserts across aromatic C–H bonds, it is quite evident that this system has promise in the activation of several types of hydrocarbon C–H bonds. Indeed, preliminary results confirm the wide applicability of the $[(NP_3)Rh]^+$ fragment to the C–H activation field: C–H bonds in alkynes, aldehydes, and olefins are readily cleaved to give stable *cis*-(σ-organyl) hydrides.[4] Attempts to functionalize the various organyl groups are presently under way.

Reductive elimination of the metalated phenyl group from **15** can also be promoted by monodentate ligands, which invariably form Rh(I) complexes. In particular, H^-, halides, and pseudohalides such as Cl^-, I^-, or N_3^- give TBP complexes of the formula $[(NP_3)RhX]$ (X = H (**7**); Cl (**1**); I (**18**); N_3 (**19**)), whereas neutral monodentate ligands such as CO and pyridine yield cationic derivatives of the formula $[(NP_3)RhX]^+$ (X = CO (**20**); pyridine (**21**)) (Scheme III). As observed for **1**, the neutral derivatives **18** and **19** are not sufficiently soluble to be characterized adequately in solution. The IR spectrum of **19** exhibits a strong absorption at 2015 cm^{-1} assigned to the stretching of the terminal azido ligand. By contrast, the cationic species **20** and **21** are soluble in THF, acetone, and halogenated hydrocarbons. The $^{31}P\{^1H\}$ NMR spectra of both compounds show splitting patterns consistent with TBP geometries. The presence of a terminal carbonyl ligand in **20** is confirmed by a strong IR absorbance at 1975 cm^{-1}.

Octahedral complexes in which the two additional coligands are disposed in mutually cis positions are obtained by reacting THF solutions of **15** with a plethora of addenda including H_2, Cl_2, and CS_2 to give *cis*-dihydride, *cis*-dichloride,[2] and η^2-CS_2[3] derivatives (Scheme III).

Unlike the NP_3 and NP_3Cy analogues **3** and **5**, the reaction of the *cis*-(hydride)chloride **4**, with an excess of $NaBH_4$, does not give a *cis*-dihydride derivative; the Rh(I) monohydride $[(PP_3)RhH]$ (**8**) is instead straightforwardly obtained in high yield. This result is not unexpected given the η^2-H_2 nature of the complex cation $[(PP_3)RhH_2]^+$ in ambient temperature solutions.[5] The latter complex loses dihydrogen either thermally or by addition of suitable substrates such as CO, halides, and H^-. Accordingly, it is reasonable to conclude that the primary product of the reaction

(47) Siedle, A. R.; Newmark, R. A.; Pignolet, L. H. *Organometallics* **1984**, *3*, 855.
(48) Andreucci, L.; Diversi, P.; Ingrosso, G.; Lucherini, A.; Marchetti, F.; Adovesio, V.; Nardelli, M. *J. Chem. Soc., Dalton Trans.* **1986**, 803.
(49) (a) Janowicz, A. H.; Bergman, R. G. *J. Am. Chem. Soc.* **1983**, *105*, 3929. (b) Wenzel, T. T.; Bergman, R. G. *Ibid.* **1986**, *108*, 4856. (c) Jones, W. P.; Feher, F. J. *Ibid.* **1985**, *107*, 620. (d) Smith, G. M.; Carpenter, J. D.; Marks, T. J. *Ibid.* **1986**, *108*, 6805. (e) Antberg, M.; Dahlenburg, L. *Angew. Chem., Int. Ed. Engl.* **1986**, *25*, 260. For review articles see: (f) Halpern, J. *Inorg. Chim. Acta* **1985**, *100*, 41. (g) Rothwell, I. P. *Polyhedron* **1985**, *4*, 177.
(50) Jones, W. D.; Feher, F. J. *J. Am. Chem. Soc.* **1984**, *106*, 1650.
(51) Lawrance, G. A. *Chem. Rev.* **1986**, *86*, 17.

of **4** with H^- is the η^2-H_2 complex, which subsequently undergoes replacement of H_2 with H^- to give the TBP monohydride **8** (Scheme VII). In nice agreement with such a mechanism we have found that when the reaction is carried out at room temperature, the formation of **8** is accompanied by $[(PP_3)RhH_2]^+$ (ca. 10%). The lower the temperature, the higher is the yield of the latter species.

Compound **8** is a yellow crystalline product that shares many chemical properties with the NP_3 analogue **7** such as a great reactivity toward electrophilic reagents. As an example, protonation of **8** by strong protic acids such as HBF_4·OEt_2 or $HOSO_2CF_3$ affords the colorless Rh(III) complex $[(PP_3)RhH_2]^+$, which can be isolated as $SO_3CF_3^-$ (**9a**), BF_4^- (**9b**), or BPh_4^- (**9c**) salts. Because of the facile dissociation of the H_2 ligand in solution, the reaction must be carried out under a H_2 atmosphere and, possibly, at low temperature, in order to get a good yield.

In the solid state (as well as in solution below 183 K), the complex cation $[(PP_3)RhH_2]^+$ exhibits OCT geometry determined by the four donor atoms of the tripodal polyphosphine and by the two hydride ligands. By contrast, as recently reported by us, it rearranges to TBP geometry at temperatures higher than 183 K as a consequence of H–H bonding. The η^2-H_2 ligand is rather labile: colorless solutions of **9a–c** under a nitrogen atmosphere progressively become reddish while hydrogen is evolved. On bubbling H_2 through these solutions, the red color rapidly vanishes to give colorless solutions from which the η^2-H_2 complex can be precipitated by adding *n*-butanol. On concentration, the reddish solutions give crystals only in the case of **9a**; those of **9b–c** afford intractable powders. The red crystals which analyze as $[(PP_3)Rh(SO_3CF_3)]$ (**24**) can be prepared also by methylation of the monohydride **8** dissolved in benzene. Like the analogous NP_3 reaction, we propose the intermediacy of an unstable *cis*-(methyl)hydride species which undergoes the reductive elimination of CH_4. Unlike the NP_3 case, the elimination of methane is not followed by cyclometalation. In fact, the IR spectrum of **24** exhibits neither ν(Rh–H) absorptions nor modification in the phenyl vibration pattern. Instead, it reveals the presence of coordinated triflate anion as shown by the intense ν(SO) absorption located at 1310 cm^{-1}.[51] The presence of coordinated triflate is supported also by the negligible conductivity of the compound in nitroethane solution as well as, indirectly, by the fact that solutions of **9b–c** do not yield a **24**-like derivative. The $^{31}P\{^1H\}$ NMR spectrum exhibits two first-order AM_2QX spin systems of equal intensities, each of which may be attributed to an isomeric form of **24**. Conceptually, an AM_2QX pattern is consistent with both OCT and square-pyramidal (SP) geometries caused by η^2(O,O)- or η^1(O)-coordination of the triflate ion, respectively. However, since a bidentate triflate ion would give rise to a 20-electron species, it is reasonable to assign to **24** a SP geometry for which two isomers may exist by η^1-coordination of the triflate ion trans either to P_A (VII) or to P_Q (VIII). Such an hypothesis is supported by the coincidence of both the chemical shifts and coupling constants of the P_M nuclei in the two patterns. Alternatively, **24** can be synthesized by reacting the methyl derivative **11** with triflic acid in THF or benzene suspension whereupon CH_4 is observed to be evolved.

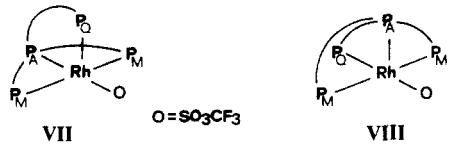

VII VIII

In contrast to the analogous NP_3 fragment, the $[(PP_3)Rh]^+$ system neither intramolecularly inserts across a C–H bond from a ligand phenyl ring nor intermolecularly activates a C–H bond from benzene. Most likely, this is a consequence of having a stronger central donor atom, phosphorus, which makes the metal more encapsulated in the natural cavity of the tripodal ligand. In other words, the PP_3 system is less open at the central atom than the NP_3 one. At least in principle, this would result in hampering the approach of a benzene molecule and, therefore, cyclometalation should be favored. On the other hand, we have

Scheme VIII

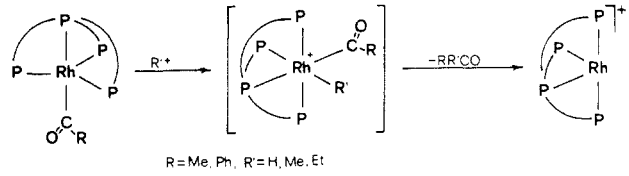

shown that PP_3 is more reluctant than NP_3 to form OCT complexes of rhodium(III): the OCT *cis*-dihydride $[(PP_3)RhH_2]^+$ rearranges to the formally Rh(I), TBP η^2-H_2 derivative in ambient temperature solutions.[5] Furthermore, we have recently reported that protonation or alkylation of the acyl complexes **13** and **14** result in the reductive elimination of aldehydes and ketones through intramolecular C–H and C–C bond formation, respectively (Scheme VIII).[52]

On going down the triad Co, Rh, and Ir, the chemistry of the 16-electron $[(NP_3)M]^+$ and $[(PP_3)M]^+$ fragments dramatically changes: the cobalt complexes are totally inactive to C–H bond activation whereas the related iridium systems easily insert across hydrocarbon sp^3 and sp^2 C–H bonds without apparent cyclometalation.[6,7] While thermodynamic constraints, notably those associated with the strength of M–C and M–H bonds, are of dominant importance in limiting the reactivity of the cobalt complexes,[49f] we interpret the preference of iridium for intermolecular reaction as due to lesser steric crowding. In this respect, it is worth noticing that a similar metal-dependent transition between intra- and intermolecular C–H activation[49e] by homoleptic Fe and Ru complexes has been discussed by Antberg and Dahlenburg in terms of steric factors, i.e., the system with the heavier element is more open at the central metal center and, therefore, more propitious for intermolecular C–H bond activation.

Compound **24** exhibits a surprisingly rich chemistry, readily undergoing oxidative addition with various inorganic and organic substrates to give octahedral complexes of Rh(III). Alternatively, neutral monodentate ligands such as carbon monoxide or triphenylphosphine react with **24** to give cationic Rh(I) complexes of the formula $[(PP_3)RhX]BPh_4$ (X = CO (**27**), PPh_3 (**28**)) by subsequent addition of $NaBPh_4$. Analogously, anionic monodentate ligands such as Cl^-, N_3^-, or H^- yield neutral TBP complexes of the formula $[(PP_3)RhX]$ (X = Cl^- (**2**), N_3^- (**26**), H^- (**8**)). With the exception of **28**, all of these compounds show ^{31}P NMR AM_3X patterns consistent with TBP geometries where the bridgehead P atom of the tripodal ligand is located in an axial position, trans to the monodentate X group. By contrast, **28** exhibits a first-order AM_3QX spin system due to the presence in an axial position of a fifth phosphorus atom provided by PPh_3. As a result, each resonance of the PP_3 phosphorus nuclei is further split into a doublet. As expected, the coupling constant $J(P_AP_Q)$ is very large since it originates from two nonequivalent phosphorus atoms lying trans to each other [$J(P_AP_Q)$ = 279.1 Hz].[36]

In addition to H_2, a great variety of substrates containing acidic hydrogens such as protic acids, BH, or alkynes with electron-withdrawing substituents, can oxidatively add to the 16-electron $[(PP_3Rh]^+$ fragment. In this way, Rh(III) *cis*-(B)hydride and *cis*-(acetylide)hydride[41] complexes are obtained. As an example, we describe here the reaction of **24** with triflic acid to give the octahedral *cis*-(hydride)triflate complex $[(PP_3)RhH(SO_3CF_3)]$-BPh_4 (**25**) that can be isolated as colorless crystals after addition of $NaBPh_4$.

Compound **25** is air-stable both in the solid state and in solution. It is soluble in common organic solvents in which it behaves as a 1:1 electrolyte. The IR spectrum exhibits a strong intensity absorbance at 1970 cm^{-1} associated with the stretch of the Rh–H bond. A medium intensity band at 1320 cm^{-1} is consistent with the presence of coordinated triflate.[51] The $^{31}P\{^1H\}$ NMR spectrum

(52) Bianchini, C.; Meli, A.; Peruzzini, M.; Zanobini, F. *Organometallics* **1987**, *6*, 2453.

Table V. Summary of Crystal Data for **17a**

formula	$C_{73.5}H_{70}B_1P_3Rh_1I_1N_1O_{0.5}$
mol weight	1308.93
cryst size, mm.	0.425 × 0.175 × 0.250
cryst system	triclinic
space group	$P\bar{1}$
a, Å	18.361 (4)
b, Å	17.069 (4)
c, Å	11.107 (3)
α, deg	90.61 (1)
β, deg	102.73 (3)
γ, deg	101.76 (3)
V, Å^3	3318.51
Z	2
d_{calcd}, g cm^{-3}	1.310
(Mo Kα), cm^{-1}	7.68
radiation	graphite-monochromated Mo Kα (λ = 0.71069 Å)
scan type	$\omega/2\theta$
2θ range, deg	5–50
scan width, deg	0.9
scan speed, deg s^{-1}	0.04
total data	11680
unique data, $I \geq 3\sigma(I)$	7094
no. of parameters	266
R	0.068
R_w	0.076
abs corr	DIFABS
transmission factors; max, min	1.089, 0.950

consists of an AM_2QX pattern typical of OCT complexes of PP_3. The ^1H NMR spectrum shows a doublet of pseudosextuplets centered at −7.43 ppm in the hydride region.

Conclusions

The geometry of the tripodal ligands NP_3 and PP_3 is such that they can occupy four contiguous coordination sites on TBP, SP, or OCT structures. By so doing, the steric relationship of the remaining coligands is fixed: in TBP and SP geometries, a fifth group is invariably located in axial and equatorial positions, respectively.

TBP complexes of rhodium(I) exert their reactivity by several pathways, including (i) attack of electrophiles at an occupied frontier σ-orbital lying in between two equatorial phosphorus atoms; (ii) creation of a free coordination site by unfastening either phosphorus (PP_3) or nitrogen (NP_3) donors; and (iii) metathetical reactions with main group organometallic reagents.

In OCT complexes of rhodium(III), the two coligands occupy mutually cis positions: the forced proximity of these groups makes the complexes particularly prone to undergo reductive elimination reactions; the resulting reduced fragments $[(NP_3)Rh]^+$ and $[(PP_3)Rh]^+$ are able to oxidatively add a plethora of inorganic and organic substrates including H–H and C–H bonds. In particular, the $[(NP_3)Rh]^+$ system can insert across arene C–H bonds in both intramolecular and intermolecular fashion. It has been found that decreasing the temperature and increasing the arene concentration favors intermolecular activation over cyclometalation.

The chemistry of the $[(PP_3)Rh]^+$ fragment is highly influenced by its tendency to adopt the trigonal-pyramidal C_{3v} conformation. As a result, OCT Rh(III) complexes easily undergo reductive elimination reactions, which may also occur with retention of the

Table VI. Final Positional Parameters for **17a**[a]

atom	x	y	z	atom	x	y	z
I	2836 (1)	4591 (1)	−390 (1)	C6,5	4772 (5)	2700 (4)	2557 (8)
Rh	2381 (1)	3175 (1)	480 (1)	C1,6	3558 (6)	4026 (5)	3399 (8)
P1	1147 (1)	3057 (1)	−706 (2)	C2,6	3672 (6)	3877 (5)	4652 (8)
P2	2922 (1)	2471 (1)	−806 (2)	C3,6	3846 (6)	4514 (5)	5537 (8)
P3	3381 (1)	3236 (2)	2196 (2)	C4,6	3905 (6)	5299 (5)	5169 (8)
N	1926 (4)	2009 (4)	1055 (7)	C5,6	3791 (6)	5447 (5)	3916 (8)
C1	696 (5)	2042 (5)	−451 (9)	C6,6	3617 (6)	4811 (5)	3031 (8)
C2	1054 (5)	1854 (5)	824 (8)	C1,7	1980 (3)	7818 (4)	11084 (6)
C3	2852 (5)	1524 (6)	−23 (9)	C2,7	1439 (3)	7332 (4)	11612 (6)
C4	2107 (5)	1331 (5)	368 (8)	C3,7	1460 (3)	6526 (4)	11765 (6)
C5	3058 (6)	2264 (6)	2816 (11)	C4,7	2020 (3)	6206 (4)	11390 (6)
C6	2213 (6)	1994 (6)	2415 (9)	C5,7	2560 (3)	6691 (4)	10862 (6)
B	1895 (6)	8754 (6)	10729 (10)	C6,7	2540 (3)	7497 (4)	10709 (6)
C1,1	1002 (5)	3664 (5)	506 (8)	C1,8	1432 (3)	9124 (4)	11680 (4)
C2,1	1677 (5)	3695 (5)	1385 (8)	C2,8	851 (3)	9531 (4)	11224 (4)
C3,1	1705 (6)	4031 (6)	2542 (10)	C3,8	468 (3)	9819 (4)	12029 (4)
C4,1	1097 (6)	4321 (6)	2743 (11)	C4,8	665 (3)	9700 (4)	13290 (4)
C5,1	459 (7)	4303 (7)	1858 (11)	C5,8	1245 (3)	9293 (4)	13746 (4)
C6,1	390 (6)	3966 (6)	690 (10)	C6,8	1629 (3)	9005 (4)	12941 (4)
C1,2	679 (4)	3292 (3)	−2216 (6)	C1,9	2771 (4)	9355 (4)	10884 (5)
C2,2	184 (4)	2694 (3)	−3043 (6)	C2,9	3115 (4)	9840 (4)	11961 (5)
C3,2	−190 (4)	2891 (3)	−4198 (6)	C3,9	3849 (4)	10306 (4)	12097 (5)
C4,2	−69 (4)	3686 (3)	−4526 (6)	C4,9	4240 (4)	10289 (4)	11156 (5)
C5,2	425 (4)	4284 (3)	−3699 (6)	C5,9	3896 (4)	9804 (4)	10079 (5)
C6,2	799 (4)	4087 (3)	−2543 (6)	C6,9	3161 (4)	9338 (4)	9944 (5)
C1,3	2342 (5)	2260 (4)	−2385 (8)	C110	1390 (3)	8710 (3)	9261 (5)
C2,3	2070 (5)	1482 (4)	−2918 (8)	C210	849 (3)	8018 (3)	8780 (5)
C3,3	1650 (5)	1356 (4)	−4139 (8)	C310	416 (3)	7981 (3)	7571 (5)
C4,3	1504 (5)	2008 (4)	−4829 (8)	C410	524 (3)	8637 (3)	6844 (5)
C5,3	1777 (5)	2786 (4)	−4297 (8)	C510	1066 (3)	9330 (3)	7326 (5)
C6,3	2196 (5)	2912 (4)	−3075 (8)	C610	1499 (3)	9367 (3)	8534 (5)
C1,4	3886 (5)	2688 (4)	−1069 (8)	C111	2009 (10)	6990 (12)	7298 (18)
C2,4	4368 (5)	2148 (4)	−793 (8)	C211	2028 (11)	6245 (12)	7254 (18)
C3,4	5088 (5)	2317 (4)	−1067 (8)	C311	2162 (10)	5871 (11)	6253 (18)
C4,4	5325 (5)	3027 (4)	−1617 (8)	C411	2235 (10)	6258 (11)	5232 (17)
C5,4	4843 (5)	3567 (4)	−1892 (8)	C511	2223 (12)	7038 (13)	5216 (20)
C6,4	4124 (5)	3398 (4)	−1618 (8)	C611	2105 (12)	7435 (13)	6334 (22)
C1,5	4350 (5)	3257 (4)	2045 (8)	C7	3482 (29)	1024 (32)	5591 (48)
C2,5	4686 (5)	3899 (4)	1445 (8)	C8	3292 (35)	110 (38)	6088 (61)
C3,5	5444 (5)	3984 (4)	1358 (8)	C9	3805 (34)	−432 (36)	6096 (55)
C4,5	5866 (5)	3427 (4)	1870 (8)	O1	3126 (24)	228 (25)	7066 (44)
C5,5	5530 (5)	2785 (4)	2470 (8)				

[a] Coordinates multiplied by 10^4, temperature factors by 10^3.

"eliminated" molecule in the fifth position of the trigonal-bipyramid (η^2-H_2 complex).

Finally, we have compared and contrasted the reactivities of a series of isoelectronic metal fragments, namely $[(NP_3)M]^+$ and $[(PP_3)M]^+$ (M = Co, Rh, Ir), toward aromatic C-H bond activation. It appears that for those systems for which C-H oxidative addition is thermodynamically allowed (Rh, Ir), steric crowding favors the intramolecular ortho-metalation reaction.

Acknowledgment. We are grateful to Prof. A. Vacca for helpful discussion and to P. Innocenti and A. Traversi for technical assistance.

Registry No. 1, 85233-90-5; **2**, 110827-50-4; **3**, 115590-80-2; **4**, 115590-82-4; **5**, 80602-44-4; **6**, 115590-83-5; **7**, 85233-91-6; **8**, 109786-30-3; **9c**, 115590-84-6; **10**, 115590-86-8; **11**, 110827-48-0; **12**, 110827-49-1; **13**, 110827-46-8; **14**, 110827-47-9; **15**, 104910-92-1; **16**, 115591-02-1; **17**, 115590-88-0; **17a**, 115591-00-9; **18**, 114900-45-7; **19**, 114900-46-8; **20**, 89530-44-9; **21**, 115590-90-4; **22**, 114900-38-8; **23**, 115590-92-6; **24** (isomer 1), 109786-34-7; **24** (isomer 2), 109837-84-5; **25**, 115590-94-8; **26**, 115590-95-9; **27**, 115590-97-1; **28**, 115590-99-3; **29**, 95911-60-7; I, 15114-55-3; II, 23582-03-8; NP_3Cy, 115562-61-3; $[RhCl(COD)]_2$, 12092-47-6; $[(NP_3)RhCl_2]BPh_4$, 85233-87-0.

Supplementary Material Available: Refined anisotropic and isotropic temperature factors (Table VII) and final positional parameters for hydrogen atoms for **17a** (Table VIII) (5 pages); listing of observed and calculated structure factors for **17a** (42 pages). Ordering information is given on any current masthead page.

Reactivity of Trimethylaluminum with $(C_5Me_5)_2Sm(THF)_2$: Synthesis, Structure, and Reactivity of the Samarium Methyl Complexes $(C_5Me_5)_2Sm[(\mu\text{-}Me)AlMe_2(\mu\text{-}Me)]_2Sm(C_5Me_5)_2$ and $(C_5Me_5)_2SmMe(THF)$[1]

William J. Evans,* L. R. Chamberlain, Tamara A. Ulibarri, and Joseph W. Ziller

Contribution from the Department of Chemistry, University of California, Irvine, Irvine, California 92717. *Received November 12, 1987*

Abstract: $(C_5Me_5)_2Sm(THF)_2$ reduces $AlMe_3$ in toluene to form $(C_5Me_5)_2Sm[(\mu\text{-}Me)AlMe_2(\mu\text{-}Me)]_2Sm(C_5Me_5)_2$ (**1**), which crystallizes from toluene in space group $P2_1/n$ with unit cell parameters a = 12.267 (3) Å, b = 12.575 (3) Å, and c = 17.131 (2) Å and z = 2 for D_{calcd} = 1.30 g cm^{-3}. Least-squares refinement of the model based on 2163 observed reflections converged to a final R_F = 5.7%. Each trivalent bent metallocene $(C_5Me_5)_2Sm$ unit in **1** is connected to two tetrahedral $(\mu\text{-}Me)_2AlMe_2$ moieties via nearly linear Sm(μ-Me)-Al linkages (175.2 (9)° and 177.8 (7)° angles). The average Sm-C(μ-Me) distance is 2.75 (2) Å. In solution, **1** is in equilibrium with the monomer $(C_5Me_5)_2Sm(\mu\text{-}Me)_2AlMe_2$. THF cleaves the bridging $AlMe_4$ units in **1** liberating $AlMe_3$ and $(C_5Me_5)_2SmMe(THF)$ (**2**). **2** crystallizes from THF/hexane in space group *Pnma* with unit cell parameters a = 18.0630 (42) Å, b = 15.6486 (39) Å, and c = 8.7678 (15) Å and Z = 4 for D_{calcd} = 1.36 g cm^{-3}. Least-squares refinement of the model based on 2087 observed reflections converged to a final R_F = 7.0%. The bent metallocene $(C_5Me_5)_2Sm$ unit is coordinated to the methyl group and to THF with Sm-C and Sm-O distances of 2.484 (14) and 2.473 (9) Å, respectively. **2** reacts with aromatic and aliphatic hydrocarbons including benzene, toluene, hexane, cyclohexane, and cyclooctane liberating CH_4 via net activation of C-H bonds. The benzene and toluene reactions form $(C_5Me_5)_2Sm(C_6H_5)(THF)$ and $(C_5Me_5)_2Sm(CH_2C_6H_5)(THF)$, respectively, in high yield. The other reactions form complex mixtures of organosamarium products. The methane generated in the reactions of **2** with deuteriated substrates is CH_4, which suggests that intramolecular formation of a spectroscopically undetected intermediate containing a metalated C_5Me_5 ring may occur before intermolecular reaction with the C-H bond. The benzene reaction has a moderate enthalpy of activation (16.5 ± 0.6 kcal/mol) and a large negative entropy of activation (−19 ± 4 eu), consistent with the "σ-bond metathesis" mechanism proposed for C-H bond activation at electron-deficient metal centers. **2** metalates pyridine-d_5 to form CH_3D, reacts with Et_2O to form $(C_5Me_5)_2Sm(OEt)(THF)$, and reacts with H_2 to form $[(C_5Me_5)_2Sm(\mu\text{-}H)]_2$. Both **1** and **2** polymerize ethylene.

The low-valent organolanthanide complex $(C_5Me_5)_2Sm(THF)_2$[2-4] has recently been shown to effect remarkable transformations of unsaturated organic substrates including CO,[5] RC≡CR,[6] RCH=CHR,[7] and RN=NR.[8] Much of the reactivity observed was unprecedented, which suggested that the full potential of $(C_5Me_5)_2Sm(THF)_2$ could best be defined by exploratory studies with a range of substrates. To expand our knowledge of the reactivity of $(C_5Me_5)_2Sm(THF)_2$, we have begun to explore reactions with organometallic and inorganic substrates. In this report, we describe the reaction of $(C_5Me_5)_2Sm(THF)_2$ with trimethylaluminum. This system provides an unusual tetrametallic $AlMe_4^-$ bridged complex and, in addition, an excellent synthetic route to the first compound containing a terminal methyl group attached to a samarium ion.[9] Both complexes function

(1) Reported in part at the 2nd International Conference on the Basic and Applied Chemistry of f-Transition (Lanthanide and Actinide) and Related Elements, Lisbon, Portugal, April 1987, L(II)1, and at the 193rd National Meeting of the American Chemical Society, Denver, CO, April 1987, INOR 227.

(2) Evans, W. J.; Grate, J. W.; Choi, H. W.; Bloom, I.; Hunter, W. E.; Atwood, J. L. *J. Am. Chem. Soc.* **1985**, *107*, 941-946.

(3) Evans, W. J. In *High-Energy Processes in Organometallic Chemistry*; K. S. Suslick, Ed.; American Chemical Society: Washington, DC, 1987; ACS Symp. Ser. No. 333, pp 278-289.

(4) Evans, W. J. *Polyhedron* **1987**, *6*, 803-835.

(5) Evans, W. J.; Grate, J. W.; Hughes, L. A.; Zhang, H.; Atwood, J. L. *J. Am. Chem. Soc.* **1985**, *107*, 3728-3730.

(6) Evans, W. J.; Hughes, L. A.; Drummond, D. K.; Zhang, H.; Atwood, J. L. *J. Am. Chem. Soc.* **1986**, *108*, 1722-1723.

(7) Evans, W. J.; Drummond, D. K. *J. Am. Chem. Soc.* **1988**, *110*, 2772-2774.

(8) Evans, W. J.; Drummond, D. K. *J. Am. Chem. Soc.* **1986**, *108*, 7440-7441.

(9) The bridging methyl samarium complex $Sm(\mu\text{-}Me)_6Li_3(Me_2NCH_2CH_2NMe_2)_3$ is known: Schumann, H.; Muller, J.; Bruncks, N.; Lauke, H.; Pickardt, J.; Schwarz, H.; Eckart, K. *Organometallics* **1984**, *3*, 69-74.

0002-7863/88/1510-6423$01.50/0